DTIC

Simulation of Sea Clutter Returns

Irina Antipov

DSTO-TR-0679

DEPARTMENT OF DEFENCE
DEFENCE SCIENCE AND TECHNOLOGY ORGANISATION

Simulation of Sea Clutter Returns

Irina Antipov

Tactical Surveillance System Division
Electronic and Surveillance Research Laboratory

DSTO-TR-0679

ABSTRACT

This report presents the results of a study, the main aim of which was proper prediction of sea clutter characteristics and modelling of sea clutter including both the temporal and spatial properties of the return signals. More detail has been given to the K-distribution as this model enables the simulation of clutter with a good level of approximation to the real data.

DEPARTMENT OF DEFENCE

DEFENCE SCIENCE AND TECHNOLOGY ORGANISATION

Published by

DSTO Electronic and Surveillance Research Laboratory
PO Box 1500
Salisbury South Australia 5108

Telephone: (08) 8259 5555
Fax: (08) 8259 6567

AR No. AR-010-560
June 1998

APPROVED FOR PUBLIC RELEASE

Simulation of Sea Clutter Returns

Executive Summary

This report represents the results of a study performed under the task ADA95/080-TSSD support for Project AIR 5276. Under this task, TSSD is providing advice to the RAAF on several aspects of the upgrade of the P3C Orions with a focus on the Israeli designed EL/M 2022 maritime surveillance radar system being installed as part of this upgrade.

The design and selection of radars and radar signal processing algorithms for use in a sea clutter environment is directly influenced by knowledge of sea clutter properties. In practice, the parameters of the amplitude distributions, correlation properties and phase characteristics of the targets and clutter are not known a priori, and a radar must adapt its processing to set the detection threshold at an appropriate level for the conditions actually encountered. Therefore it is necessary to be able to predict the range of conditions likely to be encountered, their dependence on various radar system parameters and their likely rate of change, both temporally and spatially. Robust models have been developed describing sea clutter over a wide range of operating and environmental conditions, allowing the analysis of the effects of various processing and system changes mathematically.

This report presents the results of a study, the main aim of which was proper prediction of sea clutter characteristics and modelling of sea clutter including both the temporal and spatial properties of the return signals. Amplitude, phase and correlation characteristics of the sea clutter, and different methods for the prediction of the parameters of these characteristics have been analysed.

As an accurate prediction of performance is usually more dependent on the accurate modelling of correlation features than on the choice of amplitude distribution, more attention has been given to the K-distribution model of the sea clutter. It provides a good description of the clutter amplitude statistics and has particular advantages in facilitating proper handling of the temporal and spatial fluctuations of the clutter.

The procedures for simulation of the K-distributed sea clutter with the desired parameters of the amplitude distribution and the specified temporal and spatial correlation properties have been suggested and implemented.

The analysis and comparison of the experimentally collected and synthetically generated data show that the K-distribution is the most promising model of sea clutter which simulates the clutter with a good level of approximation to the real data.

Simulators based on the developed models can be used to generate realistic sea clutter data which can be input to computer models of the radar system and the resulting performance measured.

Authors

Irina Antipov
Tactical Surveillance System Division

Dr. Irina Antipov received her degree in 1988 from St-Petersburg Academy of Aerospace Instrumentation, Russia. From 1996 she has worked in Tactical Surveillance System Division as a Research Scientist. Her research interests are in the modelling and simulation of sea clutter for a variety of purposes including: investigating the performance of maritime radar systems, adapting radar systems to operate in clutter environment, investigating concepts of operation of maritime radar systems.

Contents

1. INTRODUCTION 1

2. PREDICTION OF SEA CLUTTER CHARACTERISTICS 1
2.1 Amplitude characteristics of sea clutter 2
2.1.1 The choice of sea clutter amplitude distribution 2
2.1.2 K-distributed clutter model 4
2.1.3 Models for mean clutter reflectivity 6
2.1.4 Comparison of the mean clutter reflectivity models 8
2.1.5 Empirical models for the prediction of the shape parameter 10
2.2 Phase characteristics of sea clutter 13
2.3 Correlation properties of sea clutter 14
2.3.1 Temporal correlation properties 15
2.3.2 Spatial correlation properties 16
2.4 Prediction of the K-distribution parameters for lower resolution radar using information about these parameters for high resolution radar 18

3. SIMULATION OF SEA CLUTTER RETURNS 19
3.1 Computer generation of K-distributed radar sea clutter with specified temporal correlation properties 19
3.2 Computer generation of K-distributed radar sea clutter with specified spatial correlation properties 24
3.3 Influence of thermal noise on the amplitude distribution of sea clutter returns 28

4. IMPLEMENTATION OF SEA CLUTTER SIMULATING PROCEDURES 29
4.1 Description of the software package for synthetic generation of sea clutter returns 29
4.2 Performance results of the simulation procedures 35

5. SUMMARY 47

6. REFERENCES 48

APPENDIX 1 SIT SEA CLUTTER MODEL.....52

APPENDIX 2 GIT SEA CLUTTER MODEL.....53

APPENDIX 3 TSC SEA CLUTTER MODEL 55

APPENDIX 4 HYB SEA CLUTTER MODEL.....57

List of figures

FIGURE 1 IMPORTANT PARAMETERS FOR SEA CLUTTER SIMULATION 30
FIGURE 2 FLOW CHART SHOWING PROCEDURES FOR SIMULATION OF SEA CLUTTER RETURNS 31
FIGURE 3 FLOW CHART SHOWING PROCEDURES FOR PREDICTION OF CLUTTER AMPLITUDE CHARACTERISTICS 32
FIGURE 4 FLOW CHART SHOWING PROCEDURES FOR SIRP BASED SIMULATION OF SEA CLUTTER RETURNS 33
FIGURE 5 EXPERIMENTALLY COLLECTED SEA CLUTTER 36
FIGURE 6 TEMPORAL AND SPATIAL AUTOCORRELATION FUNCTIONS FOR EXPERIMENTALLY COLLECTED SEA CLUTTER 37
FIGURE 7 SPECTRAL ANALYSIS FOR THE RANGE BIN OF EXPERIMENTALLY COLLECTED SEA CLUTTER 37
FIGURE 8 FREQUENCY-TIME ANALYSIS FOR THE RANGE BIN OF EXPERIMENTALLY COLLECTED SEA CLUTTER 38
FIGURE 9 NORMALISED AMPLITUDE HISTOGRAM FOR A RANGE LINE OF EXPERIMENTALLY COLLECTED SEA CLUTTER 38
FIGURE 10 K-PDFS ESTIMATED BY DIFFERENT METHODS FOR EXPERIMENTALLY COLLECTED SEA CLUTTER 39
FIGURE 11 PDFS OF DIFFERENT DISTRIBUTIONS FOR EXPERIMENTALLY COLLECTED SEA CLUTTER 39
FIGURE 12 SYNTHETICALLY GENERATED SEA CLUTTER 43
FIGURE 13 TEMPORAL AND SPATIAL AUTOCORRELATION FUNCTIONS FOR SYNTHETICALLY GENERATED SEA CLUTTER 44
FIGURE 14 SPECTRAL ANALYSIS FOR THE RANGE BIN OF SYNTHETICALLY GENERATED SEA CLUTTER 44
FIGURE 15 FREQUENCY-TIME ANALYSIS FOR THE RANGE BIN OF SYNTHETICALLY GENERATED SEA CLUTTER 45
FIGURE 16 NORMALISED AMPLITUDE HISTOGRAM FOR A RANGE LINE OF SYNTHETICALLY GENERATED SEA CLUTTER 45
FIGURE 17 K-PDFS ESTIMATED BY DIFFERENT METHODS FOR SYNTHETICALLY GENERATED SEA CLUTTER 46

List of tables

TABLE 1 POPULAR MODELS FOR SEA CLUTTER AMPLITUDE DISTRIBUTIONS.....2
TABLE 2 MEAN CLUTTER REFLECTIVITY MODEL CAPABILITIES.....9
TABLE 3 WARD'S AND WICK'S MODEL CONSTANTS.....12
TABLE 4 ESTIMATES OF THE DISTRIBUTION PARAMETERS BY DIFFERENT METHODS FOR EXPERIMENTALLY COLLECTED SEA CLUTTER DATA SET.....40
TABLE 5 MODIFIED CHI-SQUARED INDEX χ_m^2 VALUES AND STANDARD DEVIATION σ_v FOR DIFFERENT ESTIMATION METHODS FOR EXPERIMENTALLY COLLECTED SEA CLUTTER DATA SET.....41
TABLE 6 ESTIMATES OF THE K-DISTRIBUTION PARAMETERS BY DIFFERENT METHODS FOR SYNTHETICALLY GENERATED SEA CLUTTER DATA SET.....43
TABLE 7 MODIFIED CHI-SQUARED INDEX χ_m^2 VALUES AND STANDARD DEVIATION σ_v FOR DIFFERENT ESTIMATION METHODS FOR SYNTHETICALLY GENERATED SEA CLUTTER DATA SET.....46
TABLE 8 SITTROP'S SEA CLUTTER MODEL CONSTANTS.....52

1. Introduction

The design and selection of radars and radar signal processing algorithms for use in a sea clutter environment is directly influenced by knowledge of sea clutter properties. In practice, the parameters of the amplitude distributions, correlation properties and phase characteristics of the targets and clutter are not known a priori, and a radar must adapt its processing to set the detection threshold at an appropriate level for the conditions actually encountered. Therefore it is necessary to be able to predict the range of conditions likely to be encountered, their dependence on various radar system parameters and their likely rate of change, both temporally and spatially. Robust models have been developed describing sea clutter over a wide range of operating and environmental conditions, allowing the analysis of the effects of various processing and system changes mathematically. In addition, simulators based on these models can be used to generate realistic sea clutter which can be input to computer models of the radar system and the resulting performance measured.

This report presents the results of a study, the main aim of which was proper prediction of sea clutter characteristics and modelling of sea clutter including both the temporal and spatial properties of the return signals. Amplitude, phase and correlation characteristics of the sea clutter, and different methods for the prediction of the parameters of these characteristics have been analysed. The procedures for simulation of sea clutter returns with specified properties have been suggested and implemented. More detail has been given to the K-distribution as the most promising model of sea clutter which allows the simulation of clutter with a good level of approximation to the real data.

2. Prediction Of Sea Clutter Characteristics

There are many natural factors that determine the characteristics of the radar backscatter from the sea, including the sea state, the wind speed, duration and direction, the wave speed, the fetch and the swell direction. There are also several radar parameters that will affect the measured backscatter including the radar carrier frequency, the bandwidth (or range resolution), antenna beamwidth, two-way antenna pattern value at the sea surface, noise temperature, pulse repetition frequency, transmitted power, receive and transmit polarisations, range to the centre of the clutter cell, and the antenna angle of incidence relative to the sea surface. The knowledge of these parameters allows the prediction of amplitude and phase characteristics of sea clutter and its temporal and spatial correlation properties.

2.1 Amplitude characteristics of sea clutter

The radar returns from the surface of the sea are noise-like spatial and temporal stochastic processes. Their characterisation is one of the central problems in optimum radar performance analysis. Unlike thermal noise, most clutter returns are correlated non-Gaussian processes. Thus, for example, high resolution, low grazing-angle sea clutter data exhibit significantly larger amplitude variances than those predicted by the Rayleigh Probability Density Function. Therefore, the Gaussian model for the inphase and quadrature components of the radar returns should be replaced with other more realistic and self-consistent statistical models that agree with the experimental data. This section of the report briefly presents the models which have been applied to sea clutter amplitude distribution and discusses the influence of different factors on the parameters of these distributions. Particular attention is paid to the K-distribution as the most promising model of sea clutter.

2.1.1 The choice of sea clutter amplitude distribution

The most popular models for describing of sea clutter amplitude distributions are: Rayleigh [1-4], Log-Normal [4-8], Weibull [4, 9-12] and K-distribution [13-20]. The model Cumulative Distribution Function (CDF) , Probability Density Function (PDF), and moments of these distributions are presented in Table 1[1]. In this table, a is the amplitude of the return signals and is defined for the range $0 \le a \le \infty$.

Table 1 Popular models for sea clutter amplitude distributions

Model	CDF	PDF	Moments
Rayleigh	$F_R(a) = 1 - \exp\{-(\frac{a}{\varpi})^2\}$	$f_R(a) = \frac{2a}{\varpi^2}\exp\{-(\frac{a}{\varpi})^2\}$	$E(a^r) = \varpi^r \Gamma(1+\frac{r}{2})$
Log-Normal	$F_L(a) = \Phi(\frac{\ln a - \mu}{\sigma})$	$f_L(a) = \frac{1}{\sqrt{(2\pi)}\sigma a}\exp\{-\frac{(\ln(a)-\mu)^2}{2\sigma^2}\}$	$E(a^r) = \exp(r\mu + \frac{1}{2}r^2\sigma^2)$
Weibull	$F_W(a) = 1 - \exp\{-(\frac{a}{\varpi})^\gamma\}$	$f_W(a) = \frac{\gamma}{\varpi}(\frac{a}{\varpi})^{\gamma-1}\exp\{-(\frac{a}{\varpi})^\gamma\}$	$E(a^r) = \varpi^r \Gamma(1+\frac{r}{\gamma})$
K-distribution	$F_K(a) = 1 - \frac{2}{\Gamma(\nu)}(\frac{ca}{2})^\nu K_\nu(ca)$	$f_K(a) = \frac{2c}{\Gamma(\nu)}(\frac{ca}{2})^\nu K_{\nu-1}(ca)$	$E(a^r) = \frac{2^r \Gamma(0.5r+1)\Gamma(0.5r+\nu)}{\Gamma(\nu)c^r}$

[1]Definitions: ϖ is a scale parameter for the Rayleigh and Weibull distributions; r is the order of moment; $\Gamma(z)$ is the Gamma function; $\ln(a)$ is Normally distributed with mean μ and variance σ^2 for Log-Normal distribution; γ is a shape parameter for the Weibull distribution; c is a scale parameter and ν is a shape parameter for the K-distribution; $K_{\nu-1}(z)$ is the modified Bessel function of the second kind of order ν and $\Phi(z) = \int_{-\infty}^{z} \frac{1}{\sqrt{2\pi}}\exp\left\{-\frac{t^2}{2}\right\}dt$.

From a review of available literature [1-20] the following conclusions can be drawn:

1) For large illuminated patch sizes and high grazing angles ($\varphi \geq 10^0$) it is found that sea clutter obeys the Central Limit Theorem and has Rayleigh distributed amplitude statistics. The range correlation is commensurate with the pulse length and, if the transmitter frequency is stepped by the pulse bandwidth each pulse, the results are independent from pulse to pulse.

2) The following conditions are known to result in echo PDFs that have longer tails and the clutter is described as "spiky":
   a) higher resolution;
   b) lower grazing angles of incidence;
   c) rougher sea states;
   d) horizontal polarisation of transmitted and received signals.

   In these cases, the amplitude statistics have been modelled by Log-Normal, Weibull and K- distributions. All these distributions can produce reasonable fits to observed clutter statistics in different conditions.

3) The Log-Normal distribution is always spikier than either K- or Weibull. At ν=0.5 the K-distribution and the Weibull are identical. Over a large range of ν they are very similar, with the K-distribution being slightly more spiky than the Weibull for larger ν and slightly less spiky for smaller ν. The K-distribution is mathematically much more difficult to work with than others.

4) The statistical results of many experiments provide evidence that the K-distribution can serve as a limiting distribution for sea clutter.

5) The K-distribution is the most appropriate model for sea clutter in the low Probability of False Alarm (PFA) region.

6) Except for the K-distribution, other non-Rayleigh distributions are not derived from a physical model or clutter scattering mechanism. Their choice and validation are based only on their agreement with experimental data. As a result, although these models of spiky sea clutter can be adequately fitted to the amplitude statistics, they do not describe the temporal and spatial correlation in the data. The fact that this problem is overcome with the K-distribution has a great importance because the accurate prediction of performance is usually more dependent on the accurate modelling of correlation features than on the choice of amplitude distribution.

These conclusions explain the reasons why the K-distribution has received widespread attention recently as a model for sea clutter. It provides a good description of the clutter amplitude statistics and has particular advantages in facilitating proper handling of the temporal and spatial fluctuations of the clutter.

2.1.2 K-distributed clutter model

The K-distribution model has its origin in the observation that, over a wide range of conditions, the sea clutter returns for high resolution radars can be well modelled by two components [15-20].

The first component is an underlying mean level obeying a generalised Chi-distribution:

$$f(y) = \frac{2d^{2\nu} y^{2\nu-1}}{\Gamma(\nu)} \exp(-d^2 y^2) \ , \tag{1}$$

where $\Gamma(\nu)$ is the Gamma function, ν is a shape parameter and d is a scale parameter such that $d^2 = \frac{\nu}{E(y^2)}$ where $E(y^2)$ is the average power of the clutter.

This mean level is a slowly varying component which can be associated with a bunching of scatterers corresponding to the gross wave structure of the sea surface. It has a long temporal decorrelation period (a correlation time of the order of seconds) and is unaffected by frequency agility. The slowly varying component has considerable spatial correlation which displays periodic effects and is coupled to the temporal correlation.

The second component is termed the 'speckle' and its amplitude is Rayleigh distributed:

$$f(a|y) = \frac{a\pi}{2y^2} \exp(-\frac{a^2\pi}{4y^2}) \ , \tag{2}$$

where y is the underlying mean level determined by (1).

The speckle is a fast varying component which can be identified with the changing interference between capillary wave scatterers. The speckle has a correlation time of the order of milliseconds, and can be decorrelated using frequency agility. This fast varying component has spatial correlation commensurate with the pulse length and is in all ways similar to noise-like clutter as its amplitude distribution confirms.

The overall amplitude of the clutter thus obeys a K-distribution given by

$$f_K(a) = \int_0^\infty f(a|y) f(y) dy = \frac{2c}{\Gamma(\nu)} \left(\frac{ca}{2}\right)^\nu K_{\nu-1}(ca) \ , \tag{3}$$

where $K_{\nu-1}(z)$ is an ν^{th}-order modified Bessel function of the second kind and $c = \sqrt{\pi} d$ is a scale parameter.

According to (3) the K-distribution is a form of modulated Gaussian distribution: a Gaussian process is modulated by a process whose PDF is a generalised Chi-distributed. This equates to modulating the power of the Rayleigh envelope of the Gaussian signal with a Gamma-distributed variable. When applied to radar sea clutter, this represents the case where the clutter amplitude in a given resolution cell exhibits rapid Rayleigh fluctuations, the mean power of which varies in time with a slow fluctuation rate, and from one resolution cell to the next, according to the Gamma distribution.
If the sea clutter amplitude has a K-distribution, the mean clutter power value is defined by relation:

$$P_c = \frac{4\nu}{c^2} . \tag{5}$$

The shape parameter ν defines the spikiness of sea clutter: the less is the value of this parameter, the more spiky is sea clutter. In practice, the value for this parameter of the distribution varies between the values of 0.1, corresponding to very spiky data and 20, corresponding to approximately Rayleigh distributed data.

The scale parameter c is responsible for the power characteristic of returned echo signals: the less is value of the scale parameter, the more powerful are reflected signals from the sea surface. For the distribution with the shape parameter ν, the scale parameter can be predicted from a knowledge of the clutter reflectivity and the radar parameters:

$$c = \sqrt{\frac{4\nu}{P_t G_t^2 \frac{\lambda^2 f^4}{(4\pi)^3 R^3} (\sigma_0 \theta_B \frac{c_l \tau_{pulse}}{2})}} , \tag{6}$$

where P_t is the transmitted power, G_t is the transmit gain, λ is the radar wavelength, f^4 is the two-way antenna pattern value at the surface, R is slant range to the clutter cell, θ_B is the antenna pattern beamwidth, τ_{pulse} is the pulse width, c_l is the speed of light and σ_0 is the mean clutter reflectivity value.

Several empirical models for the prediction of the clutter envelope distribution parameters have been derived, including models for clutter reflectivity and the K-distribution shape parameter [21-32]. These models are useful in providing guidance on the range of values likely to be encountered rather than providing any precise insight into the various parametric dependencies.

2.1.3 Models for mean clutter reflectivity

Several models of a mean clutter reflectivity, σ_0 have been developed based on different analytical methods in electromagnetic scattering theory which are applicable to the analysis of scattering from ocean waves [2,3,22]. These models use a lot of simplifying assumptions and can be used for prediction of the mean clutter reflectivity only for limited number of possible situations. Thus, the models do not provide good results for horizontal polarisation at low grazing angles because of the lack of useful analytical techniques for these kind of situations. Clearly, the scattering mechanism at microwave frequencies is complex and complicated further by multiple scattering on the sea surface. The present theoretical knowledge of ocean backscatter at microwave frequencies is not sufficiently advanced such that the magnitude of sea clutter return may be accurately predicted from purely analytical considerations. As a result, a number of semi- empirical models for the sea clutter reflectivity calculation have been developed. The approach is to define the theoretical relationship among model parameters, and use actual data to derive the model constants. This semi-empirical approach has been used by Sittrop (SIT) [23]; the Georgia Institute of Technology (GIT) [24]; the Technology Service Corporation (TSC) [25] and Dockery (HYB) [26]. The following sections briefly describe the models and their overall capabilities.

1) SIT

Sittrop provides an empirical model for the calculation of ocean mean clutter reflectivity and its spectral width at X- and Ku- bands. His model, described in detail in Appendix 1, gives the value of the mean clutter reflectivity as a function of wind speed and grazing angle, and assumes that sea clutter is entirely caused by wind generated capillary waves. Sittrop argues that the wind speed can only be related to sea state, representing specific wave heights if the wind has been steady for several hours, in a 'fully developed' sea. However, if the wind ceases to blow, these wave heights remain for a certain time, but the capillary waves die out almost instantly. This effect will have an immediate impact on the clutter return which will reduce accordingly. Hence a determination of sea clutter based on sea state observations may result in too low values of the mean clutter reflectivity if the wind speed has reduced, but the wave height has remained the same. Consequently sea clutter description is expected to be more reliable when wind speeds are used rather than sea states, in particular under diminishing wind conditions. Sittrop therefore recommends the use of wind speed over sea state for prediction of sea clutter returns, especially for the situation of abating wind. Sittrop's model provides estimates of sea clutter reflectivity for upwind and crosswind look directions and horizontal (HH) and vertical (VV) polarisations. Sittrop compares his model with the data presented by Nathanson [2] and concludes that his model is in good agreement, especially for the lower grazing angles and higher sea states.

2) GIT

The GIT model is the best known example of attempts to produce models which combine empirical factors with mathematical models of the various mechanisms involved in the backscatter of energy from the sea surface. The Georgia Institute of Technology has developed a deterministic parametric model for the mean sea clutter reflectivity, described in detail in Appendix 2, which is a function of grazing angle, wind speed and/or average wave height, angle between wind direction and antenna boresight, radar wavelength, and polarisation. In this case the mean clutter reflectivity is broken down into three factors: an interference (multipath) factor, a wind speed factor and a wind (sea) direction factor. The first factor is a theoretically derived factor for multipath interference for a Gaussian distribution of wave heights. The second and third factors were derived empirically. The wind direction factor describes the variation due to aspect angle between the antenna and sea direction.

A significant feature of the GIT model is the usage of both wave height and wind speed, permitting a more complete description of the ocean conditions. As mentioned before, one of the most complex problems in defining the sea conditions is the interaction between the wind and the swell. The time taken for a swell to develop is very much longer than the time for the wind to alter direction. In the GIT model, wind and sea directions are assumed to be highly correlated, as are wind speed and average wave height. However, for changing conditions, wind speed and average wave height could be considered as separate data. The wave height is used to introduce an interference effect due to multipath propagation that will cause faster clutter fall off at low grazing angles. This low angle fall-off is governed by a factor which is controlled by wave height, has a behaviour similar to the spherical earth propagation factor, and forces a transition in range dependence from R^{-3} to R^{-7}. If a particular grazing angle is in the R^{-3} range dependence region then further increases in wave height will have no effect on clutter amplitude at that grazing angle.

The GIT model can be used over a broad frequency range (1-100 GHz) and provides full direction dependence from upwind to downwind.

3) TSC

The Technology Service Corporation developed a model that is based on a fit to data compiled by Nathanson [2]. This model, described in detail in Appendix 3, is a function of grazing angle, Douglas sea state number, wind aspect angle, radar wavelength, and polarisation. The TSC model is similar to the GIT model in functional form and has comparable capabilities. However, several constants, and dependencies of some variables, are slightly different. The TSC model includes anomalous propagation data, so it does not fall off as rapidly with range as GIT model. In this model an effective wind speed and wave height are calculated using Douglas sea state number. However there is an option to input these two parameters independently. The TSC model can be used over a broad frequency range (0.5-35 GHz) and provides full

direction dependence from upwind to downwind. This model assumes the Nathanson's data is the average of all look directions, and as a result, treats the data as crosswind. The TSC model results for crosswind direction are in close agreement to these data.

It was suggested [22] that for cautious performance prediction or when propagation conditions are unknown, it may be better to use the TSC model rather than the SIT or the GIT models because it more closely represents average conditions.

4) HYB

The hybrid (HYB) model that includes work by Barton [27], summaries Nathanson's data [2] and features of the GIT model. This model, described in detail in Appendix 4, also takes into account the fact that Nathanson's data have been averaged over all wind directions. The mean clutter reflectivity using the HYB model is calculated by adding to the reference reflectivity of sea state 5, grazing angle 0.1^0, vertical polarisation and upwind look direction four decibel adjustments for arbitrary values of the sea state, grazing angle, polarisation and look direction. A transitional grazing angle is based on the definition of the GIT model and Barton's results. A polarisation adjustment has been taken directly from the GIT model, which was developed as an empirical fit to the Nathanson's data.

2.1.4 Comparison of the mean clutter reflectivity models

Table 2 summarises the model capabilities. All the models exhibit a number of similar trends:

1) The mean clutter reflectivity increases with sea state, frequency, and grazing angle.

2) The grazing angle dependence is particularly strong at low grazing angles.

3) The mean clutter reflectivity decreases as the look direction moves away from the upwind direction.

4) The mean clutter reflectivity value for vertical polarisation is generally greater than for horizontal polarisation, particularly for low sea states. As sea state increases, the reflectivity for horizontal polarisation may exceed that for vertical polarisation, particularly at low grazing angles.

The models are in reasonable agreement for higher grazing angles (ie those greater than 3^0) and higher sea states, but the GIT and SIT models give values consistently lower than the TSC and HYB models for low grazing angles and low sea states. At small angles, reflectivity in the GIT model varies approximately as φ^4 where φ is the grazing angle; the relationship is closer to φ^2 in the other models.

The reasons for such differences can be explained by differences in the data from which the model constants were derived. Thus, it was indicated that much of the data presented in [2] and hence the models derived from it (TSC, HYB) may be biased high in the low grazing angle range. There are two main sources of this bias. The first is related to the fact that much of the earlier sea clutter data was collected using low power radars and as a result only the clutter having sufficiently high clutter-to-noise ratio provided useful data points. The second and more significant source of the bias is ducting, which is believed to be a major contributor to sea clutter at very low grazing angles [28-30]. The records for GIT model were culled of any ducting. The other empirical models provide a fit to mean clutter cross-section measurements obtained under a variety of conditions that include ducting.

Table 2 Mean clutter reflectivity model capabilities

Parameter	Model			
	SIT	GIT	TSC	HYB
Indicated carrier frequency, GHz	9.3, 17	1 - 100	0.5 - 35	0.5 - 35
Environment:				
Average wave height (m)	No	0 to 4	Douglas sea state	Douglas sea state
Wind (kts)	< 40	3 - 30	(0 - 5)	(0 - 5)
Geometry:				
Grazing angle (degrees)	0.2 -10	0.1 - 10	0.1 - 90	0.1 - 30
Look angle (degrees)	0, 90	0 - 180	0 - 180	0 - 180
Polarisation	HH, VV	HH, VV	HH, VV	HH, VV
Input model parameters:				
Radar wavelength	Yes	Yes	Yes	Yes
Polarisation	Yes	Yes	Yes	Yes
Sea state	No	No	Yes	Yes
Wind speed	Yes	Yes	No	No
Average wave height	No	Yes	No	No
Grazing angle	Yes	Yes	Yes	Yes
Wind aspect angle	Yes	Yes	Yes	Yes

It is important to realise that the spread in values of the mean clutter reflectivity observed between the various models for a given set of conditions is not dissimilar to that which might be encountered in practice, especially given the difficulty in characterising the actual sea conditions [21]. The value of these models lies in their use for radar design. They allow the expected range of the mean clutter reflectivity values to be determined. In the case of constant false alarm rate detection, a radar has to adapt its threshold according to the spatial variations of reflectivity and the corresponding clutter amplitude statistics. The mean clutter reflectivity models described above provide good estimates of the range of values of the mean clutter reflectivity likely to

be encountered in different conditions and the expected variation with radar parameters and viewing geometry.[2]

2.1.5 Empirical models for the prediction of the shape parameter

Another important parameter to investigate is the shape parameter ν of the K-distribution, which provides information about the amplitude statistics (particularly spikiness) and also some of the correlation properties. Only a limited number of empirical models exist for the prediction of this parameter and all of them have been developed for X-band.

An empirical model was developed by Ward [17,31], relating this parameter to the grazing angle, the cross-range resolution, the sea swell direction and polarisation. This model was derived from data obtained from a radar having a 30 ns pulse length (a radar range resolution of 4.2 m) and, in its original form, vertically polarised returns. Later it was validated for horizontally polarised returns as well. The parametrization of the shape parameter has been achieved by matching the spread of results to a simple functional form and presented by formula:

$$\log(\nu) = \frac{2}{3}\log(\varphi) + \frac{5}{8}\log(l) + \delta - k \ , \tag{7}$$

where

ν is the estimated value of the shape parameter,

l is the cross-range resolution,

φ is the grazing angle in degrees ($0.1^0 < \varphi < 10^0$),

δ introduces the aspect dependency as follows:

$\delta = -\frac{1}{3}$ for up or down swell directions;

$\delta = +\frac{1}{3}$ for cross-swell directions;

$\delta = 0$ for intermediate directions or when no swell exists,

k describes the polarisation effects with $k = 1$ for vertical and $k = 1.7$ for horizontal polarisation.

According to [32], the variation with swell direction can also be approximated by a cosine function:

$$\delta = -\frac{1}{3}\cos(2\theta) \ , \tag{8}$$

[2]At this stage it is necessary to analyse existing sea clutter data which were collected by the Defence Science and Technology Organization in Australia during several trials in order to clarify what sea clutter model provides the best results for Australian environmental conditions.

where the angle θ is zero when the boresight is pointed in the direction of propagation of the swell.

The main conclusions from analysis of this empirical model for the shape parameter are:

1) for horizontal polarisation the value of the shape parameter is lower than for vertical polarisation for the same set of environmental and radar parameters. It means that with horizontal polarisation, the clutter is spikier and pulse to pulse correlation is greater than with vertical polarisation in similar conditions;

2) a small grazing angle implies smaller shape parameter;

3) there is no strong statistical trend with sea state, wind speed or aspect angle relative to wind direction;

4) aspect angle variation depends on the swell and long wavelength sea wave content of sea spectrum: smaller values of the shape parameter are characterised for up and down swell directions, larger values are usual for across swell direction and medium values of the shape parameter are typical for the intermediate directions;

5) at different ranges, the cross-range patch size is different due to the antenna footprint; there is a strong trend for increased values of the shape parameter with increased patch size;

6) since each parameter is matched separately to variations with the shape parameter, complex interdependencies may be missing.

Although theoretical considerations indicate that the shape parameter is dependent on the range resolution this model does not include such effect. As an initial guide to the range of values expected, the relationship between the shape parameter and range resolution is of the same form as that with the cross-range resolution. However, the precise relationship is more complex and depends on the relative scaling of the radar pulse length and the spatial correlation of the clutter returns, which will in turn often be determined by the sea swell wavelength [33]. Thus, the trend is for the shape parameter to increase with patch size, ie the clutter becomes less spiky, approaching a Rayleigh distribution, but the precise relationship changes according to changing spatial correlation properties associated with the wave and swell structure of the sea.

A second empirical model for the shape parameter has been proposed by Ward and Wicks [32]. Further data has been collected with the same range resolution, and added to on the original data base used to generate the first model, allowing the new empirical model to be developed. In this case least squares fits have been made separately for up/down swell and cross-swell directions, and for horizontally as well as vertically polarised data. The results are of the form:

$$\log(\nu) = A\log(\varphi) + B\log(l) + C \ , \tag{9}$$

with the values *A*, *B* and *C* being presented in Table 3, where the following definitions were used: U/D - up or down swell direction; X - cross-swell direction, H - horizontal polarisation, V - vertical polarisation.

Comparison of the two models shows that the new model provides a wider spread of values of the shape parameter for the same values of grazing angle and cross-range resolution than was observed in the original model. The disadvantage of the second model is that it does not allow the prediction of the shape parameter for intermediate directions. Also, the root-mean-square error in log(ν) is greater for the second empirical model than for the first [32].

Table 3 Ward's and Wick's model constants

Polarisation	Swell	*A*	*B*	*C*	Comments
H	U/D	0.402	0.461	-1.135	150m<*l*<300m
H	X	0.250	0.790	-1.833	150m<*l*<300m
V	U/D	0.834	0.707	-1.304	
V	X	1.040	1.227	-2.418	

These empirical models of the shape parameter are strictly only for a radar operating with a pulse length of about 30 ns (a radar range resolution of about 4 m). An attempt was made by Ryan and Johnson [34] to use additional data for different pulse lengths to modify the Ward model to include a pulse dependence; the range resolution was found to have the most dominant effect on the shape parameter, with the shortest pulse giving the smallest value of the shape parameter. The modified Ward model is given by:

$$\log(\nu) = \frac{2}{3}\log(\varphi) + \frac{5}{8}\log(l) + \delta - k + \log(\frac{\tau_{pulse}}{30})\log(\frac{50}{\varphi})\log(5.5\varphi)^{0.8} \ , \tag{10}$$

where τ_{pulse} is pulse length in nanoseconds.

This model allows the prediction of the shape parameter for radars operating with a pulse length longer than 30 ns. While the modified model appears to fit the data considered by authors very well, further validation is required using additional data sets.

Unfortunately, no models have been developed yet for a radar range resolution less than 4 m. Therefore, it remains necessary to validate the existing models for such cases using collected data sets.

2.2 Phase characteristics of sea clutter

Consider now the extension of the compound K-distribution description to the case of coherently detected radar sea clutter. A coherent radar measures the complex received signal rather than just the magnitude. Coherent detection of radar sea echo allows motions to be evaluated by determining the rate of change of phase. In this way coherent processing may additionally be exploited to measure both ocean surface characteristics and to discriminate targets from clutter by virtue of their relative velocities.

It is generally accepted that the phase component of sea clutter is Uniformly distributed on 2π [16]. This follows from the fact that the sea clutter return is a result of the interacting returns of a very large number of individual reflectors distributed over the area of the surface within the range cell being considered.

The combined return from a large number of ever-changing reflectors on a patch of the sea surface is subject to very complex constraints on motion and this is reflected in the observation of complicated motion-related (ie Doppler) characteristics of sea clutter: the Doppler spectrum of sea clutter is much wider than, for example, the Doppler spectrum of ground clutter, and is non-stationary.

One explanation for the frequency spread of signals returned from sea clutter is that the distribution of radial velocities of the scatterers causes a distribution of Doppler frequencies [3]. These scatterers may be either individual wavelets, wind-blown spray and foam at higher sea states, gravity waves and swell, or any combination of these. When the spread of the velocity distribution increases, such as when the surface of the sea becomes more agitated, the clutter spectrum also broadens. It was shown [3], that an almost linear dependence of bandwidth on wind speed or sea state exists. Attempts to derive differences in upwind, downwind, and crosswind spectral widths proved inconclusive. At this time, it is assumed that spectral width is independent of wind direction.

Experimentally collected sea clutter data exhibits a complex relationship between the local intensity and the spectral shape. The modulation of intensity is a result of changes in the integrated power of the spectrum as a function of time. However, according to published results of sea clutter studies [15, 17], the normalised form of the spectrum is not constant, but has a changing shape and Doppler shift. While the intensity modulation is dominated by the swell structure in the sea surface, the form of spectrum is additionally affected by the local gusting of the wind.

Generally, the time averaged spectrum of sea clutter is asymmetrical, with a bias towards positive or negative Doppler frequencies and a longer spectral tail in the direction of the Doppler shift. This bias is associated by some researchers with the direction of the prevailing wind blowing above the sea surface [17]. On the other hand, some others reported that there was no consistent correlation between the recorded wind direction and the direction of maximum Doppler shift in the sea clutter

throughout the experiment period and suggested that the observed Doppler shift was at least partly the result of ocean current, which was known to be present in the area of experiments [4].

Significantly, there is no assurance that sea clutter observed in the presence of ocean currents will be similar to that observed from a wind driven sea surface. Nevertheless, it would be qualitatively informative to compare the results assuming similar sea conditions. The reasoning is that in an open ocean a sea wave travelling in a given direction could be a result of a steady wind blowing in the same direction.

Thus, it was reported that for both sea and ocean observations, the mean Doppler shift of the averaged spectrum is significantly different for horizontal and vertical polarisations: in all cases, except that of crosswind, the Doppler shift for a horizontal polarisation sea clutter spectrum is greater than that for vertical polarisation for similar sea conditions, suggesting that a different set of scatterers are contributing to the received signals. More detailed analysis of the dependency of the Doppler shift of the averaged spectrum for both polarisations on the direction of look of the radar with respect to the sea surface is presented in [17]. According to the results of this analysis, data for both polarisations show a cosinusoidal dependence on the direction of the wind, with a zero Doppler shift when looking across-wind. This conclusion is in agreement with observations reported by some other authors.

The results of experimental measurements [15, 17] show, that despite the complexity of the phase characteristics of sea clutter , the compound form of the K-distribution is still applicable for the description of statistical properties of high resolution, coherently detected sea clutter.

It can be readily shown that the statistical distribution for inphase and quadrature components arising from the K-distributed envelope PDF is a generalised Laplace distribution [15]:

$$f(a_I) = f(a_Q) = \frac{2b^{\nu/2+1/4}}{\Gamma(\nu)\pi^{1/2}} a_{I(Q)}^{\nu-1/2} K_{\nu-1}(2a_{I(Q)}\sqrt{b}) \quad , \tag{11}$$

where a_I is the amplitude of the inphase component, a_Q is the amplitude of the quadrature component, b is a scale parameter and ν is a shape parameter.

2.3 Correlation properties of sea clutter

It is well understood that sea clutter models based only on single-point statistics (eg the amplitude distribution) are misleading in that most detection algorithms use temporal or spatial signal processing. In order that the performance prediction be correct, the correlation functions used in the model must comply with those obtained from experimental data. As mentioned before, one of the greatest advantages of the K-

distribution model is that it provides the foundation for a full quantitative treatment of correlation. The following sections of the report discuss temporal and spatial correlation properties of the sea clutter and show how they can be taken into account in this model.

2.3.1 Temporal correlation properties

The return observed from a single resolution cell containing sea clutter is generally not independent from pulse to pulse.

The form of the correlation between pulses is described by the use of the composite model: over a short period the reflected signals from any clutter resolution cell are always Rayleigh-distributed, indicating a return from multiple scatterers, and this speckle component has a Chi-distributed underlying mean level, which characterises, for example, the mean level variation of clutter spikes or the periodic variation in amplitude seen when looking up or down the sea swell.

The speckle component from any individual resolution cell has a short temporal decorrelation period (typically a few milliseconds) and is fully decorrelated pulse to pulse by frequency agility. In contrast, the mean level has a long temporal decorrelation period and is not affected by frequency agility.

Therefore, the temporal autocorrelation function of the sea clutter has a fast drop-off which is followed by a slower periodic decay [15, 17].

If sea clutter signals reflected from the individual resolution cell are observed and processed on time intervals much shorter than the average decorrelation time of the modulating process (as is actually the case for many operational radar systems), then according to the composite scattering model the return strength of these signals is proportional to the sea clutter radar cross-section per unit area, but is essentially constant during the time a single resolution cell is illuminated. Thus the modulating process exhibits negligible temporal fluctuations within the radar coherent processing interval or dwell. In this case the overall correlation properties of the returned signals are dictated by those of the rapidly varying component of the sea clutter.

If the sample mean of the time series from an individual resolution cell (which has short duration compared to the average decorrelation time of the modulating process) is first removed before correlation is performed, the autocorrelation function of the speckle component can be found:

$$ACF_k = \frac{\sum_{n=0}^{N-1} x_n x_{n+k}^*}{\sum_{n=0}^{N-1} x_n x_n^*}, \qquad (12)$$

where * denotes the complex conjugate; x_n is the complex received signal

$$x_n = a_n \exp(j\theta_n) \ , \tag{13}$$

$$a_n = \sqrt{x_{cn}^2 + x_{sn}^2} \ , \tag{14}$$

$$\theta_n = \arctan(\frac{x_{sn}}{x_{cn}}) \ , \tag{15}$$

where a_n and θ_n are the envelope magnitude and phase of the quadrature components, respectively, and subscripts c and s denote the in-phase and out-of-phase quadrature components.

For a symmetrical clutter spectrum, centred about zero Doppler, this autocorrelation function is a real and even function [4]. If the spectrum has a net Doppler shift, the autocorrelation function is the product of the real function from the zero-Doppler-shift case with a complex sinusoid $\exp(\pm j\omega_d T)$, where ω_d is the angular Doppler frequency and T is the time lag. The sign in the complex sinusoid is associated with the direction of the Doppler shift. Therefore, for a symmetrical sea clutter spectrum that can be represented by a Gaussian function, the spectral width and the Doppler shift can be determined from the autocorrelation function. As sea clutter spectra are seldom symmetrical, the following empirical relationships, which have been found to work reasonably well for X and S-bands [4], are used:

1) the 3 dB spectral width of the sea clutter is approximately equal to the inverse of twice the decorrelation time. The decorrelation time of the sea clutter has to be obtained by measuring the time it takes the envelope of the sea clutter correlation function (for the speckle component) to decay to $1/e$ of its peak value, where e is the base of the natural logarithm;

2) the Doppler shift has to be estimated using the period of the modulating sinusoid for the autocorrelation function (for the speckle component). This period is determined from the distance of the second zero-crossing of the imaginary part from the origin. The imaginary part of the autocorrelation function starts at zero, and the point of the second zero-crossing represents a full period.

2.3.2 Spatial correlation properties

The spatial correlation of sea clutter is defined as the cross correlation between the signals returned from two separate patches of the sea in the radial dimension. The time interval separating the measurement of these two signals is assumed to be so small that there is negligible time decorrelation [3].

Spatial correlation of sea clutter reflected signals is a well-known phenomenon [3, 33, 35, 36], caused by the relation of the sea clutter modulating process to the surface profile of the sea. While microwave signals are primarily scattered by capillary waves

of the sea (speckle), the undulating structure of the sea gravity waves causes variations in the mean power scattered from a given patch (modulating process), which are mechanistically explained in terms of bunching of contributing scatterers and local tilting of the mean surface slope. Therefore, it is reasonable to assume that the degree of correlation of the modulating process between resolution cells depends on the spatial correlation of the sea surface, and that this process has a decorrelation distance of the same order of magnitude as the decorrelation distance of the sea. It is also clear, that in well developed swell conditions, a periodic component will be present in the spatial autocorrelation function of the modulating process. Concerning the correlation properties of the speckle, it is necessary to note that, for a given realisation of the large scale structure, the small scale features at two spatially separated patches are usually uncorrelated - so, the speckle is assumed to be entirely decorrelated from one range cell to the next.

As a result, the overall spatial autocorrelation function is given by the sum of two terms: a spike at the origin and a scaled version of the autocorrelation function of the modulating process, from which it may be concluded that the spatial correlation characteristics of the sea clutter are solely dependent on the modulating component.

Sometimes it is more convenient for the purposes of analysis and modelling to use the spatial autocorrelation function of the mean clutter reflectivity rather than the spatial autocorrelation function of the modulating process (ie clutter mean level). According to the compound K-distribution model, the average clutter reflectivity, τ_i, in any one range cell can be expressed in terms of the local mean level y_i of the clutter as [33]

$$\tau_i = 4\frac{y_i^2}{\pi} = \bar{a_i^2} \ , \tag{16}$$

where $\bar{a_i^2}$ is the squared amplitude of the reflected signal averaged over number of successive pulses from i^{th} range cell.

The spatial autocorrelation function of the clutter mean reflectivity can be estimated from the experimentally collected data by using the following procedure [33]:

1) the radar returns from each transmitted pulse are recorded as a series of samples in range: a_i , $i=1,2,...,M$, where a_i is the amplitude of the received signal for i^{th} range sample number;

2) each point in range is averaged by integrating successive returns from the same range, decorrelated, either temporally or by using frequency agility, in order to remove the speckle component of the clutter, and yield profiles of the mean level y:

   $y_i = \bar{a_i}$, $i=1,2,...,M$. The integration period is assumed to be short compared with the correlation period of the underlying mean clutter level;

3) the average reflectivity at each range $\tau_i = \bar{a}_i^2$, $i=1,2,...,M$ is estimated by squaring these data;

4) the spatial autocorrelation function of the clutter mean reflectivity is estimated for a number of profiles using

$$SACF_j = \frac{\sum_{i=1}^{M/2}(\tau_i - \hat{m})(\tau_{i+j} - \hat{m})}{\sum_{i=1}^{M/2}(\tau_i - \hat{m})^2} , \qquad (17)$$

where $\hat{m} = \frac{1}{M}\sum_{i=1}^{M}\tau_i$ and M is the number of range samples in each profile.

5) the final spatial autocorrelation function of the clutter mean reflectivity is obtained by averaging equation (17) over groups of successive profiles of the mean clutter reflectivity.

Note that it may be quite difficult to accurately estimate the spatial autocorrelation function from short data records.

2.4 Prediction of the K-distribution parameters for lower resolution radar using information about these parameters for high resolution radar

The data reported in the literature [33,36] indicate that any variation in radar resolution results in a corresponding variation of the shape parameter of the generalised Chi-distribution of the sea clutter modulating process. It was also shown, that the returns from groups of m correlated, identically K-distributed resolution cells can be related to a single return from a single resolution cell m times larger, whose clutter mean level component is Chi-distributed with a shape parameter dependent upon the spatial correlation of the original cells. As the distribution of the clutter speckle component remains unchanged with radar resolution, the distribution of the overall clutter envelope is still K-distributed, but with different shape and scale parameters.

Thus, if parameters of the distribution and spatial correlation of the underlying mean level for the high resolution radar are known, this information may be used to estimate the model parameters of clutter for different resolution cell sizes, as the range resolution is reduced. The results of this study would be particularly useful for extending the applicability of data recorded at a particular resolution to provide clutter statistics at different resolution.

Assuming that the echo from each resolution cell for a high resolution radar is modelled by a K-distribution with the shape parameter ν and the scale parameter c, and that the m echo amplitudes are correlated, the estimates of the characteristics of echo from a large resolution cell which comprises all the m smaller cells are given by [36]

$$\nu_m = \frac{1}{\alpha - 1} \quad , \tag{18}$$

$$c_m = c\sqrt{\frac{\nu_m}{m\nu}} \quad , \tag{19}$$

$$\alpha = \frac{1}{m}\frac{\nu+1}{\nu}\left[1 + 2\sum_{i=1}^{m-1}(1-\frac{i}{m})SACF_i\right] \quad , \tag{20}$$

where ν_m is the shape parameter and c_m is the scale parameter of the K-distribution of the overall echo amplitude.

The problem of using the formulas (18) - (20) is that the compound clutter model may not be applicable to resolution cell areas below a certain lower limit. There exists no published results at the present time to suggest a value for this limiting size. It is important to note also, that these formulas are only valid for the class of clutter modelled by the K-distribution.

3. Simulation Of Sea Clutter Returns

Representative clutter models are important in evaluating radar detection performance, particularly in radars that employ constant false alarm rate processors to adapt the detection threshold to the local background noise or clutter power. Temporal and spatial correlation of the sea clutter affects constant false alarm rate detection performance, the analysis of which therefore requires techniques for describing and simulating temporally and spatially correlated clutter.

So, radar returns from the sea surface must be statistically modelled for radar performance to be predicted and for radar parameters and signal processing optimisation in a maritime environment. In order to do this correctly, it is necessary to develop realistic models of sea clutter based on estimated real data statistics.

3.1 Computer generation of K-distributed radar sea clutter with specified temporal correlation properties

As clutter can be highly correlated, realistic modelling of the clutter returns involves incorporating the correlation information into the joint probability density function

(PDF) of the clutter sample. In the simplest case of statistically independent returns, the joint PDF is simply the product of the marginal PDFs. Modelling dependent non-Gaussian clutter is however a very difficult problem, which is equivalent to the problem of generating random variables with a jointly specified marginal PDF and covariance matrix. It is straight forward to control either the PDF or the correlation function but it is more difficult to control both of them simultaneously. This problem can be solved by using one of the two following procedures:

1) zero memory nonlinear (ZMNL) transformations on a correlated Gaussian sequence to obtain the desired non-Gaussian sequence [5, 7, 9-11, 14];

2) applying the theory of spherically invariant random processes (SIRPs) [37-42].

Using ZMNL transformations on a correlated Gaussian sequence does not offer a practical solution to the joint problem for several reasons:

- as the covariance matrix of the non-Gaussian sequence is related to that of the Gaussian sequence in a rather complicated manner, it is not always possible to determine the corresponding covariance matrix of the Gaussian sequence for given a certain covariance matrix of the non-Gaussian sequence;

- if the Gaussian sequence at the input of the nonlinear transformation is bandlimited, the output is also bandlimited if and only if the nonlinearity is a polynomial. Moreover, for input Gaussian processes, any ZMNL transformation smooths and broadens the output spectrum;

- ZMNL transformation approaches do not afford independent control of the marginal PDF and correlation function;

- the nonlinear transformation imposes a specific relationship between the covariance matrix at its input and output. Therefore, given a covariance matrix at the output of the nonlinear transformation, the nonnegative-definite property of the covariance matrix at the input is not guaranteed

In contrast, the theory of SIRPs provides mathematically tractable techniques to construct multivariate non-Gaussian PDFs: the PDF of every random vector obtained by sampling a SIRP is uniquely determined by the specification of a mean vector, a covariance matrix, and a characteristic first-order PDF.

A SIRP is a special case of an exogenous product model, which agrees with the composite scattering theory for sea clutter with K-distributed amplitude, and according to which the clutter is modelled as a zero-mean complex correlated Gaussian process $v(t)$, modulated by a real, non-negative, stationary non-Gaussian process $y(t)$, independent from $v(t)$: $x(t) = y(t)v(t)$. The modulating process $y(t)$ is assumed to have a much longer decorrelation time than $v(t)$, and change little over

short time spans. The complex correlated Gaussian process $v(t)$ may be modelled as a complex white Gaussian process $w(t)$ filtered through a linear (possibly time-varying) system, whose impulse response is determined by the correlation properties of $v(t)$.

The main feature of this model is that it allows independent control of the amplitude PDF, which is dictated by the first-order PDF $f(y)$ of the modulating process $y(t)$, and of the correlation properties, which are essentially those of the Gaussian process $v(t)$. In [39] it is shown that, according to the total probability law, the envelope $a(k) = y(k)|v(k)|$ of the resulting sequence has the marginal PDF

$$f_A(a,k) = \int_0^\infty \frac{a}{y^2\sigma^2(k)} \exp(-\frac{a^2}{2y^2\sigma^2(k)}) f(y) dy \quad , \tag{21}$$

where $\sigma^2(k)$ is the mean square value of the clutter quadrature components and $y(k)$ has been assumed, without loss of generality, to have unit root mean square value.

Therefore, the amplitude distribution is uniquely determined by the marginal PDF $f(y)$ of the modulating process $y(k)$. Moreover, because $y(k)$ and $v(k)$ are independent, the complex correlation function of $x(k)$ is given by

$$ACF_x(n,m) = ACF_y(m) ACF_v(n,m) \quad , \tag{22}$$

where $ACF_y(m)$ is the autocorrelation function of $y(k)$ and $ACF_v(n,m)$ is the complex autocorrelation function of $v(k)$. Since $ACF_y(m) \approx 1$ for any m where $ACF_v(n,m)$ is not vanishingly small, the overall correlation properties of $x(k)$ are approximately those of the underlying Gaussian sequence.

The appropriate $f(y)$ for the K-distribution is a generalised Chi-PDF [39]:

$$f(y) = \frac{2\nu^\nu}{\Gamma(\nu)} y^{2\nu-1} \exp(-\nu y^2) \quad . \tag{23}$$

For time periods, whose duration is short compared to the decorrelation time of the modulating process $y(k)$, the overall process $x(k)$ can be generated by the product of a Gaussian process $v(k)$ and a modulating random variate y, rather than a modulating random process $y(k)$: $x(k) = yv(k)$. This replacement leads to a SIRP.

The multivariate PDF of the complex SIRP $x(k)$ is given by

$$f_{\mathbf{x}}(\mathbf{x}) = (2\pi)^{-N}|\mathbf{M}|^{-1/2}\int_0^\infty y^{-2N}\exp\left[\frac{-(\mathbf{x}-\mathbf{m})^T\mathbf{M}^{-1}(\mathbf{x}-\mathbf{m})}{2y^2}\right]f(y)dy\ , \tag{24}$$

where

$\mathbf{x} = \|x_{c1},\ldots,x_{cN},x_{s1},\ldots,x_{sN}\|^T$ is a $2N$-dimensional vector whose elements are N samples from the inphase and quadrature components;

$\mathbf{m}$ and $\mathbf{M}$ are the average and the covariance matrices of $\mathbf{x}$, respectively.

Due to the structure of $\mathbf{x}$ its covariance matrix takes on the form

$$\mathbf{M} = \begin{bmatrix}\mathbf{M}_{cc} & \mathbf{M}_{cs}\\ \mathbf{M}_{sc} & \mathbf{M}_{ss}\end{bmatrix}, \tag{25}$$

where $\mathbf{M}_{cc}$ and $\mathbf{M}_{ss}$ are the covariance matrices of the inphase and quadrature components, respectively, and $\mathbf{M}_{cs}$ and $\mathbf{M}_{sc}$ are their crosscovariance matrices.

According to [40], certain conditions need to be satisfied when x(t) is a wide-sense stationary SIRP:

- the quadrature components must have zero mean;
- the envelope of the pairwise quadrature components must be statistically independent of the phase, and the phase is Uniformly distributed over the interval (0, 2π). This results in the pairwise quadrature components being identically distributed and their joint PDF being circularly symmetric. This also results in the orthogonality of the pairwise quadrature components at each sampling instant;
- the autocorrelation function and crosscorrelation function of the quadrature processes of the complex process $x(t) = x_c(t) + jx_s(t)$ must satisfy the conditions given by

$$ACF_{cc}(\tau) = ACF_{ss}(\tau)\ , \tag{26}$$

$$ACF_{cs}(\tau) = -ACF_{sc}(\tau)\ , \tag{27}$$

where $ACF_{aa}(\tau) = E[x_a(t)x_a(t-\tau)]$ and $ACF_{ab}(\tau) = E[x_a(t)x_b(t-\tau)]$. Also, the nonnegative-definite property of the correlation matrix of x must be satisfied.

Clearly, if sea clutter is observed and processed on time intervals much shorter than the average decorrelation time of the modulating process (large-scale phenomenon), then it can be considered as a SIRP to a reasonable degree of approximation [38].

A mathematical model for the high-resolution radar sea clutter, which takes into account the variations of the average backscatter coefficient, is obtained by assuming that the value of this coefficient is constant in a given resolution cell, and hence in intervals of duration of T corresponding to the illumination time, but varies from cell to cell according to the PDF $f(y)$ of the modulating process $y(t)$.

In a short-time simulation by block of length N, a complex N-dimensional vector has to be generated, whose components are samples from the complex envelope of the clutter process, or, equivalently, a $2N$-dimensional real vector, whose components are samples from inphase and quadrature components of the clutter.

As the closed form of the characteristic PDF is known for K-distributed sea clutter and since an efficient algorithm producing the Chi-distributed variable y exists [39], the simulation procedure based on following steps can be implemented:

1) generate a random variable y from the characteristic PDF $f(y)$ given by (23);

2) generate a $2N$-dimensional white zero-mean Gaussian random vector $\mathbf{W}$, having identity covariance matrix;

3) perform the linear transformation to obtain the $2N$-dimensional spherically invariant random vector (SIRV) $\mathbf{V}$ with the desired covariance matrix given by

$$\mathbf{V} = \mathbf{G}\mathbf{W} , \tag{28}$$

where

$$\mathbf{G} = \mathbf{E}\mathbf{D}^{\frac{1}{2}} , \tag{29}$$

$\mathbf{E}$ is the matrix of normalised eigenvectors of the covariance matrix $\mathbf{M}$,
$\mathbf{D}$ is the diagonal matrix of eigenvalues of $\mathbf{M}$,

4) obtain N-dimensional vectors of the Rayleigh-distributed envelope $\mathbf{U}$ and the uniformly distributed phase $\mathbf{F}$ of the quadrature components of the vector $\mathbf{V} = [\mathbf{V}_c \quad \mathbf{V}_s]^T$:

$$\mathbf{U} = \sqrt{\mathbf{V}_c^2 + \mathbf{V}_s^2} , \tag{30}$$

$$\mathbf{F} = \arctan(\frac{\mathbf{V}_s}{\mathbf{V}_c}) . \tag{31}$$

5) generate the product given by $\mathbf{A} = y\mathbf{U}$ to obtain N-dimensional vector of the K-distributed amplitude of the sea clutter with desired correlation properties.

Note, that the N-dimensional complex vector X is determined by

$$\mathbf{X} = \mathbf{A}\exp(j\mathbf{F}) , \tag{32}$$

and its quadrature components, which have the generalised Laplace distribution, can be found using well-known formulas:

$$\mathbf{X}_c = \mathrm{Re}\{\mathbf{X}\} \text{ and } \mathbf{X}_s = \mathrm{Im}\{\mathbf{X}\} .$$

According to the simulation procedure, the average power σ^2 of the quadrature components is equal to unity. In order to obtain the quadrature components with the average power $\sigma^2 > 1$, it is necessary to perform the transformation:

$$\mathbf{X}_\sigma = \sqrt{\frac{2\nu}{c^2}}\mathbf{X} . \tag{33}$$

3.2 Computer generation of K-distributed radar sea clutter with specified spatial correlation properties

As it was shown in the SIRP method, which is based on the compound approach, the Gaussian noise is filtered and then modulated by the process with the Gamma-distributed power to provide a K-distribution for the amplitude. So, this technique introduces the non-Gaussian property through the Gamma modulation. Therefore, it is necessary to develop an efficient algorithm for modelling of a correlated Gamma-distributed process with desired spatial correlation properties.

To analyse directly the effects on constant false alarm rate detection performance of the correlated Gamma-distributed modulation process with arbitrary autocorrelation function, the n-th order multivariate Gamma distribution is required. No unique representation of such a multivariate Gamma distribution exists, with several alternative representations being available [14, 19, 43]. The generalised multivariate Gamma distribution representation is applicable to modelling of the modulating process, but unfortunately for $n > 2$ the mathematics becomes exceedingly complicated, even before compounding with the speckle is attempted.

Considering the slowly varying modulating component in detail, it has been found that approximating this component from its first- and second-order statistics alone provides a reasonable fit to the experimentally collected data.

In [44] a method of generating spatially correlated clutter based on linear filtering of an uncorrelated gamma process has been described. This yields the correct modulation process spatial autocorrelation function, but the resulting clutter is not exactly K-distributed and consequently has incorrect higher order moments.

In [45] a method for the simulation of correlated K-distributed clutter that involves applying moving average filters to sequences of independent Gamma-distributed variables has been proposed. The resulting sequences are summed to obtain the required correlation properties. Unfortunately this procedure becomes increasingly complex as the correlation length (or non-zero lag) increases.

In [46] a procedure which yield precisely K-distributed samples of arbitrary spatial autocorrelation function has been presented. The key advantages of this procedure are:

1) the spatial correlation is introduced to Gaussian processes, thus enabling well established linear filtering techniques to be used;

2) the resulting clutter process is strictly K-distributed;

3) it leads to useable expressions for the multivariate description of the modulation and clutter processes.

The procedure is based on a compound clutter model according to which K-distributed clutter is represented as the product of a Rayleigh speckle component and the square root of a Gamma-distributed modulation process:

$$a = y\upsilon = \sqrt{\tau}\upsilon \ , \tag{34}$$

where a is the amplitude of the K-distributed clutter, υ is the Rayleigh speckle amplitude, y is the Chi-distributed amplitude envelope modulation process, and τ is the Gamma-distributed power modulation process.

As the speckle is modelled as being independent in adjacent range cells, then the spatial correlation properties are solely dependent on the modulating gamma component.

From probability distribution theory, if τ is Gamma-distributed with shape parameter ν , then if $\nu = {}^{(m+1)}\!/_{2}$, m = 0, 1, 2,..., the PDF of τ reduces to the Chi-Square distribution, which can be generated as the sum of squares of $n = 2\nu$ independent zero-mean Gaussian processes, g_i. Correlation of the modulation process can then be introduced on the constituent Gaussian processes by well established linear filtering techniques, and the correlated Gamma component can be obtained as the sum of the squares of a small number of Gaussian components with the same autocorrelation function.

The correlation between the two gamma variables τ_1 and τ_2 is obtained from $E(\tau_1\tau_2)$, where $E(.)$ denotes expectation, such that [46]

$$E[(\tau_1\tau_2)^m] = \int_0^\infty \int_0^\infty (\tau_1\tau_2)^m f_{\tau_1\tau_2}(\tau_1,\tau_2)d\tau_1 d\tau_2 \ , \tag{35}$$

where

$m = \frac{1}{2}$,1 for the voltage and power modulation processes, respectively;

$f_{\tau_1,\tau_2}(\tau_1,\tau_2)$ is the bivariate Gamma PDF of the modulation process:

$$f_{\tau_1,\tau_2}(\tau_1,\tau_2) = \frac{1}{2^{\nu+1}\rho^{\nu-1}(1-\rho^2)\Gamma(\nu)}(\tau_1\tau_2)^{\frac{(\nu-1)}{2}} \exp\left\{-\frac{\tau_1+\tau_2}{2(1-\rho^2)} I_{\nu-1}\left[\frac{\rho\sqrt{\tau_1\tau_2}}{1-\rho^2}\right]\right\} \ , \tag{36}$$

$$\tau_j = \sum_{i=1}^{n} g_{ij}^2 \ , \quad \text{for} \quad j=1,2; \tag{37}$$

$G_i = \{g_{i1}, g_{i2}\}$ for i=1,...,n is the sample of n independent unit variance zero-mean Gaussian vectors with the correlation factor between corresponding samples $E(g_{i1}g_{i2}) = \rho$;

$I_n(x)$ is the modified Bessel function of the first kind of order n.

Each of τ_1,τ_2 is Chi-Square-distributed with n degrees of freedom. Substituting (36) into (35) gives for $0 < \rho < 1$

$$E[(\tau_1\tau_2)^m] = \frac{2^{2m}(1-\rho^2)^{\nu+2m}}{\Gamma(\nu)} \sum_{i=0}^{\infty} \rho^{2i} \frac{[\Gamma(\nu+i+m)]^2}{\Gamma(\nu+1)\Gamma(\nu+i)} \ . \tag{38}$$

For $\rho = 0$ the value of $E(\tau_1\tau_2) = 4\nu^2$ and for $\rho = 1$ the value of $E(\tau_1\tau_2) = 4\nu(\nu+1)$. This gives the correlation coefficient $\rho_{\tau_1\tau_2}$ between two samples of the modulating process in terms of the correlation coefficient ρ between corresponding samples of the constituent Gaussian process:

$$\rho_{\tau_1\tau_2} = \frac{E(\tau_1\tau_2) - E(\tau_1)E(\tau_2)}{\sqrt{V(\tau_1)}\sqrt{V(\tau_2)}} \ . \tag{39}$$

If ρ is varied as a function of the lag $k = |i-j|$ between the samples g_{i1} and g_{i2} (and consequently between τ_1 and τ_2), then equation (38) can be used to describe the spatial autocorrelation function of τ in terms of that of the g_i. A numerical approach can be used for the reverse operation of (38) as usually an analytical solution is not available. If m = 1, (38) yields the invertible expression for the spatial autocorrelation function of τ as

$$R_{\tau\tau}(k) = 4\nu\{[R_{gg}(k)]^2 + \nu\}\ , \tag{40}$$

$$\rho_{\tau\tau}(k) = \frac{R_{\tau\tau}(k) - |E(\tau)|^2}{\sigma^2(\tau)} = R_{gg}^2(k)\ , \tag{41}$$

where $R_{gg}(k)$ is the autocorrelation function for the g_i.

Thus, the correlation coefficient between the two Gamma variables corresponds to the square of the correlation coefficient of the Gaussian components used to generate the Gamma variable.

The preceding derivations can be generalised by letting ν take on arbitrary positive values $\nu \neq \frac{(m+1)}{2}$, where m is an integer. Because it is impossible to have a non-integer number of constituent Gaussian processes, a memoryless nonlinear transformation is required to transform a Chi-Square-distributed process τ with n degree of freedom ($n = 2\nu'$ and $\nu' = {}^{(m+1)}\!/_{2}$), into a Gamma-distributed process τ'' with shape parameter ν ($\nu \neq \frac{(m+1)}{2}$), that is $\Gamma(b,\nu)$ where b is any desired scale parameter. The required transformation in the case of n=2 is given by the following equation [46], which must be solved for τ'' in terms of τ

$$\tau = -2\ln\left[1 - \frac{1}{\Gamma(\nu)}\gamma(\nu, \frac{\tau''}{b})\right], \tag{42}$$

where $\gamma(.)$ is the Incomplete Gamma function.

Therefore, for integer or semi-integer values of the shape parameter ν, the modulation process is generated as the sum of the squares of a number ($n = 2\nu$) of independent zero-mean Gaussian processes, each of which has its autocorrelation determined from (41).

Obtaining a Gamma-distributed process of arbitrary ν ($\nu \neq \frac{(m+1)}{2}$) includes two stages:

1) the modulation process τ is generated as the sum of the squares of two independent zero-mean Gaussian processes, each of which has its autocorrelation determined from (41);

2) this process τ is used for a nonlinear transformation procedure (determined from (42)) to obtain a Gamma-distributed process for arbitrary ν. The nonlinear

transformation is organised by numerically solving equation (42) for every sample of the process τ .

An important advantage of this model is that the spatial correlation is introduced to Gaussian processes, thus enabling any required autocorrelation function to be obtained while a Gamma distribution for the resulting process is maintained.

The K-distributed clutter is obtained by multiplying the spatially correlated modulation $y = \sqrt{\tau}$ with the speckle, onto which the desired temporal correlation properties have been imposed.

3.3 Influence of thermal noise on the amplitude distribution of sea clutter returns

The presence of thermal noise in the radar receiver, which in general cannot be neglected, modifies the distribution of the received signals. According to published results [43, 47], the distribution of K-distributed clutter combined with additive thermal noise is not K-distributed and a closed-form expression defining this distribution does not exist.

Assuming that the noise takes the form of an uncorrelated zero-mean Gaussian process added to the received signals before processing, the mean-square power level of this noise is defined by relation [3]

$$P_n = kT\Delta f \ , \tag{43}$$

where k is the Boltzmann's constant [equal to $1.38 * 10^{-23}\, W/(Hz)(^0\, K)$], T is the system noise temperature, Δf is the noise bandwidth of the receiver after amplification but before envelope detection.

The system noise temperature includes the antenna temperature, environmental effects, and the noise of the receiver itself.

In most computations the noise bandwidth is assumed to be $1/\tau_{pulse}$, where τ_{pulse} is the pulse duration, unless more exact calculations are necessary. In distributed clutter environment calculations, the effective pulse duration τ_{pulse} should be used for more accuracy [3].

The clutter to noise ratio (CNR) is given by

$$CNR = \frac{P_c}{P_n} \ , \tag{44}$$

where P_c is the mean-square power level of the clutter.

If the simulated data has a low clutter to noise ratio (CNR < 10 dB), then the resulting amplitude distribution will be significantly altered from a standard K-distribution [47] and the low amplitude values of the clutter amplitude distribution will be the most affected by this noise: for small values of the amplitude the additive noise increases the final power significantly while for large values it leaves the power almost unchanged. Furthermore, the amplitude is concentrated about its mean value for large values of the shape parameter ν with a low probability for small values of the amplitude. Thus the added noise makes little difference to the final distribution. However, for small values of the shape parameter ν the amplitude distribution is very spiky with a high probability for small values of the amplitude. These are affected considerably by additive noise.

The noise + clutter samples are generated by adding the inphase and quadrature components of a complex valued Rayleigh random variable to the respective components of a complex valued K-distributed random variable.

4. Implementation of sea clutter simulating procedures

This section of the report describes the software package for synthetic generation of sea clutter returns that has been based on the results of the previous sections. A comparison is made of a single experimentally collected data set with the output of the model, which uses the same parameters as were estimated for the data set. The software package is a part of the MATLAB based sea clutter analysis tool which was developed in the TSSD DSTO in order to analyse the properties of sea clutter over a wide range of radar system and environmental parameters. This tool provides a relatively simple basis upon which to test new and existing radar processing and detection methods on both experimentally collected and synthetically generated sea clutter data.

4.1 Description of the software package for synthetic generation of sea clutter returns

The software package consists of:

1) an interface for entering the parameters of the simulation;

2) a section for generating the clutter, the output of which is the array of raw complex I and Q data for the K-distributed model of the sea clutter;

3) a graphical display of the data, which presents an image of the generated amplitude returns;

4) a section for different types of data analysis: correlation properties analysis, statistical analysis (histogram and distribution analysis - estimation of the parameters of the sea clutter distribution using different methods) and spectral analysis (spectrum characteristics and frequency-time domain analysis (20 points FFTs)).

Figure 1 schematically presents the parameters that are needed for proper simulation of sea clutter returns. Some of these parameters are radar system parameters such as antenna gain, beamwidth, radar frequency, polarity, transmitted power, noise temperature, bandwidth, PRF, grazing angle, two-way antenna pattern value at the sea surface, range resolution and range to centre of clutter cell. Others are environmental parameters responsible for the sea clutter characteristics: sea state for a "fully arisen" sea under conditions of stationary equilibrium, or wind velocity and average wave height for the conditions of changing wind; swell direction relative to the wind direction and look direction relative to the wind direction. All these parameters should be defined and entered using the created interface before the sea clutter generation starts.

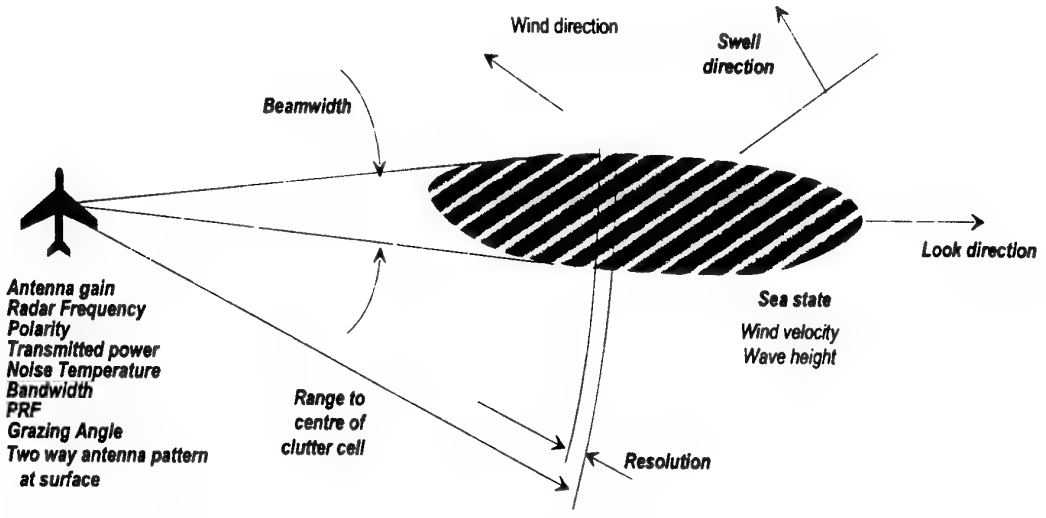

Figure 1 Important parameters for sea clutter simulation

Figure 2 illustrates the sequence of actions in calling the procedures used in the package for generation of the clutter data sets. The process of simulation can be split into four main stages:

1) prediction of clutter amplitude characteristics (magnitude and distribution);

2) prediction of clutter correlation characteristics;

3) SIRP based simulation of clutter with desired parameters and correlation properties;

4) addition of thermal noise to formed sea clutter data.

The block diagram presented in Figure 3 shows the order of calling of the procedures for prediction of clutter amplitude characteristics. This process includes:

1) prediction of the average radar cross-section per unit area σ_0 using one of the established sea clutter models (SIT, GIT, TSC or HYB);

2) prediction of the K-distribution shape parameter, ν, using one of the existing empirical formulas given by Ward, Watts and Wicks, or Ryan and Johnson [31, 32, 34];

3) calculation of the average clutter power at the receiver according to the radar equation;

4) calculation of the K-distribution scale parameter c using the relationship between the K-distribution parameters and clutter power at the receiver.

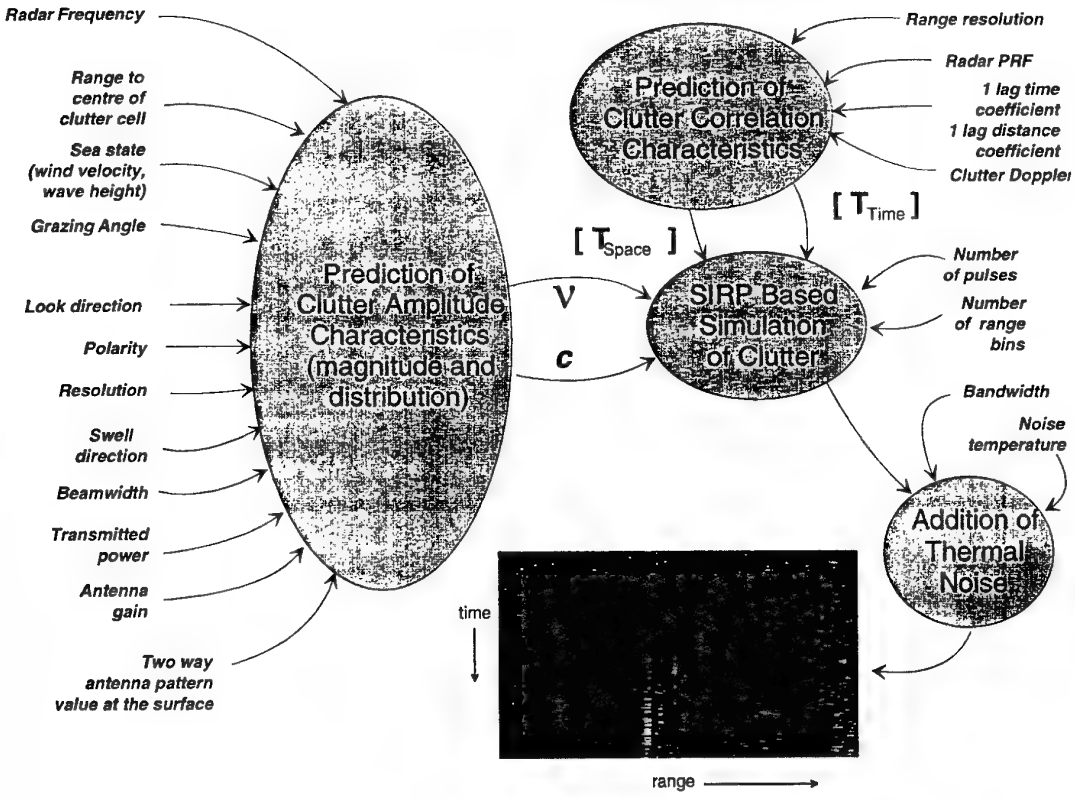

Figure 2 Flow chart showing procedures for simulation of sea clutter returns

Prediction of clutter correlation characteristics is based on the analysis of experimentally collected data for the similar conditions to those which are chosen for simulation.

The package can simulate both temporally uncorrelated and correlated sea clutter returns. In the case of temporal correlated data, the temporal autocorrelation function and its parameters have to be defined. The current version of the package gives the following choice of descriptions of temporal autocorrelation function:

$$TACF_1(\tau) = \rho_t^{\left|\frac{\tau}{\Delta t}\right|} \exp(j\omega_d \tau) \ , \tag{45}$$

$$TACF_2(\tau) = \rho_t^{(\frac{\tau}{\Delta t})^2} \exp(j\omega_d \tau) \ , \tag{46}$$

where ρ_t is the one-lag correlation coefficient for the temporal autocorrelation function, τ is the time lag, Δt is the value of time sample step, and ω_d is the angular Doppler frequency.

It is possible to use a temporal autocorrelation function derived from experimentally collected data.

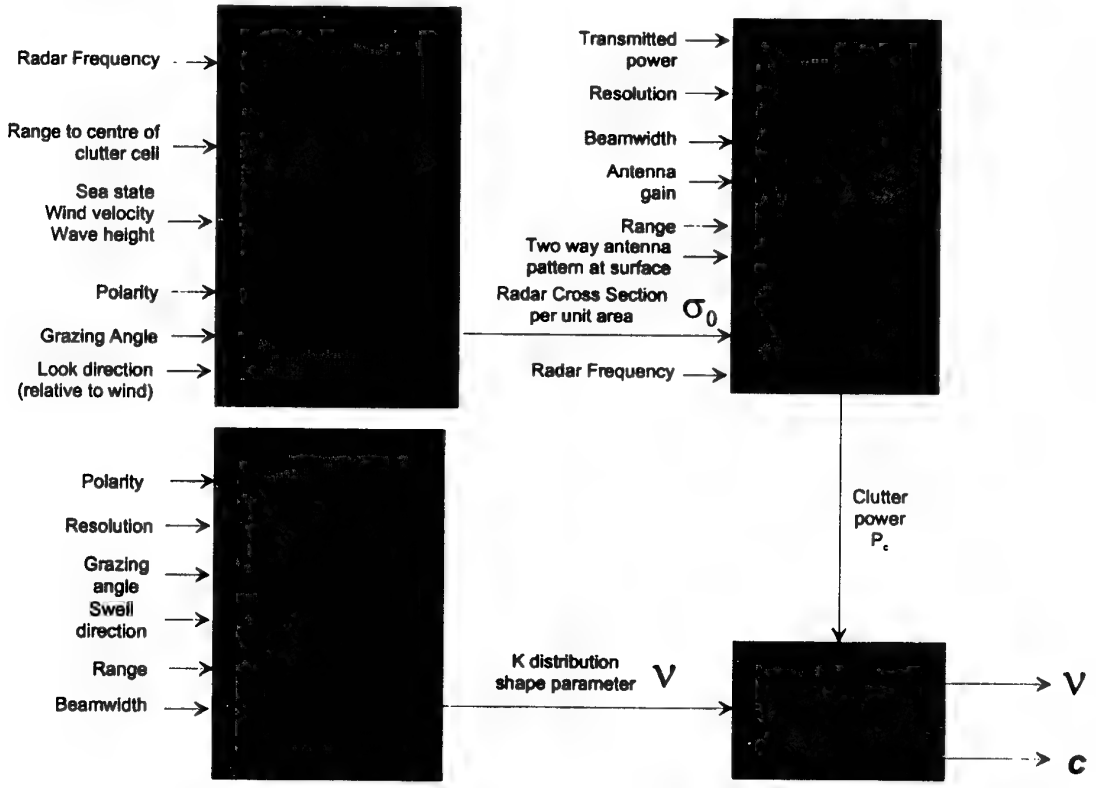

Figure 3 Flow chart showing procedures for prediction of clutter amplitude characteristics

Analogously, both spatially uncorrelated and correlated sea clutter returns can be simulated. In the case of spatial correlated data, the spatial autocorrelation function and its parameters have to be defined. The current version of the package gives the following choice of descriptions of spatial autocorrelation function:

$$SACF_1(r) = \rho_\gamma^{\left|\frac{r}{\Delta r}\right|}, \tag{47}$$

$$SACF_2(r) = \rho_\gamma^{(\frac{r}{\Delta r})^2}, \tag{48}$$

where ρ_γ is the one-lag correlation coefficient for the spatial autocorrelation function, r is the distance and Δr is the value of range resolution.

It is also possible to use a spatial autocorrelation function derived from experimentally collected data.

Figure 4 shows the order of calling of procedures for SIRP based simulation of sea clutter returns. The model of sea clutter presented by this figure has a physical interpretation in the light of the composite scattering theory, according to which the predetection clutter can be viewed as a Gaussian random process, resulting from diffusion by a large number of elementary scatterers, modulated by a highly correlated process which accounts for the gross reflectivity characteristics of the illuminated patch.

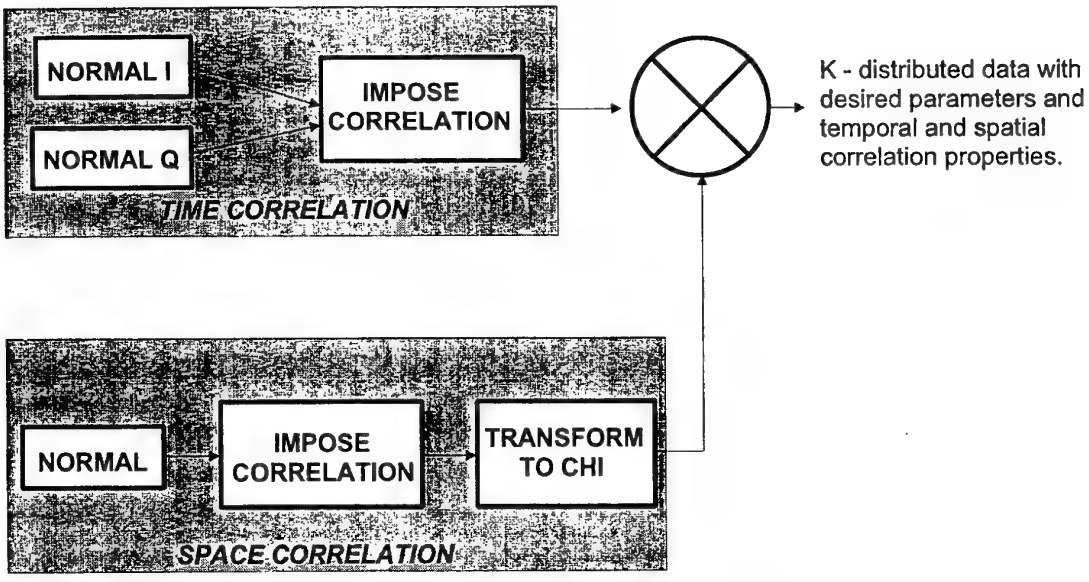

Figure 4 Flow chart showing procedures for SIRP based simulation of sea clutter returns

If this compound process is observed by windows much shorter than the average decorrelation time of the modulating process, so that this process is constant inside any window, then the model of Figure 4 applies with the modulating process degenerating into the modulating variate, changing from window to window. With this approximation the temporal correlation properties of the compound process for each range cell coincide with those of the underlying Gaussian process. So, once the spatially correlated Chi-distributed sequence of the modulating variate for the simulating number of range bins has been obtained, the effect of coherent imaging can be simulated by generating for each sample in the sequence a new temporally correlated samples from a Rayleigh distribution with mean equal to the original sample value. This process models the effect of spatially uncorrelated multiplicative speckle noise and produces K-distributed samples. The spatial correlation properties of the new process will be the same as those of the Chi-distributed process apart from a spike at zero lag in spatial autocorrelation function arising from the spatially uncorrelated speckle.

Therefore, the designed process for the simulation of the sea clutter returns, based on this approach, starts from the procedure of forming of the generalized Chi-distributed data with the chosen spatial correlation properties. The generation of the correlated data with such a distribution has been described in detail in section 3.2 of this report. Note, that in the case of the modelling of spatially uncorrelated Chi-distributed data, the much more simple procedure is used [39]. This procedure is based on well-known fast methods of generating the Gamma-distributed data. Then the theory of SIRPs is applied in order to form the desired temporal correlation properties. All stages of this procedure have been described in section 3.1 of this report. Note, that in the case of the modelling of temporally uncorrelated data, the covariance matrix $\mathbf{M}$ (25) has a diagonal structure:

$$\left\|M_{cc}\right\|_{ij} = \left\|M_{ss}\right\|_{ij} = \begin{cases} 1, i = j \\ 0, i \neq j \end{cases}, \tag{49}$$

$$\left\|M_{cs}\right\|_{ij} = \left\|M_{sc}\right\|_{ij} = 0 \ . \tag{50}$$

As a result of these steps we get an array of raw complex I and Q data for the K-distributed model of the sea clutter.

The final step in the simulation process is addition of thermal noise to the sea clutter data. The power of noise is chosen according to the desired value of the clutter-to-noise ratio.

4.2 Performance results of the simulation procedures

Before generating the K-distributed synthetic sea clutter returns, it is necessary to define all parameters responsible for the different properties of the signals: shape and scale parameters, Doppler frequency, temporal and spatial autocorrelation functions, clutter-to-noise ratio. To verify the correct functioning of the package, we analysed an experimentally collected sea clutter data set using the INGARA radar system, and deduced the underlying shape, scale and other statistical parameters. We then generated a data set using the same parameters, and compared the overall properties with the original data set.

The INGARA radar system was developed within the Tactical Surveillance Systems Division of DSTO as a technology demonstrator aimed at investigating and demonstrating the application of Synthetic Aperture Radar to the unique surveillance challenges posed by the large sparsely populated areas across the Northern Australian coastline. The main sensor of the INGARA system is a coherent, horizontal polarised, X-band multi-mode radar system. The flexible nature of the design of this radar system, based on open architectures, has allowed for the addition of maritime surveillance modes specifically designed to collect radar backscatter from the surface of the ocean (sea clutter).

The data set that has been chosen, was taken from the database of experimental data, which were collected between 9 and 11 November 1993 at Port Noarlunga South, South Australia, using the INGARA radar system at frequency of 9.375 GHz . For this trial the radar was set up on a cliff-top approximately 30 m above the sea surface. Most of the data consists of files containing 30 seconds of data, collected with the radar pointed in 15^0 intervals in azimuth angle between each data run. The azimuth angular range of the measurements was from 210^0 to 345^0.

The chosen data set consists the data for the antenna looking at an angle of 330^0. The measured meteorological conditions were :

- Wind Speed 5.9 m/s
- Wind Direction 116^0
- Air Temperature 15.7^0 C
- Sea Temperature 18.6^0C
- Relative Humidity 55.6
- Barometric Pressure 1014

Observations of the sea made from the radar site note that it was slight, with small wind ripples, probably sea state 2.

The INGARA radar coherently samples data at a 50 MHz rate (3 m in range). Each sample is a 4-byte word that represents the HI and HQ returned signals at a particular sample instant (ie. each channel is digitised to 8 bits). The symbols HI and HQ refer to the horizontal polarised inphase and quadrature channels, respectively.

An image of the amplitude of the clutter for the data set used in the analysis is presented in Figure 5. Each range window of the image represents 300 consecutive range samples, a 900m span, and the time duration is approximately 0.3 s with a PRF of 333.3 Hz. The distance from the radar to the first range bin is 3384 m. The data has been normalised to have unit second sample moment.

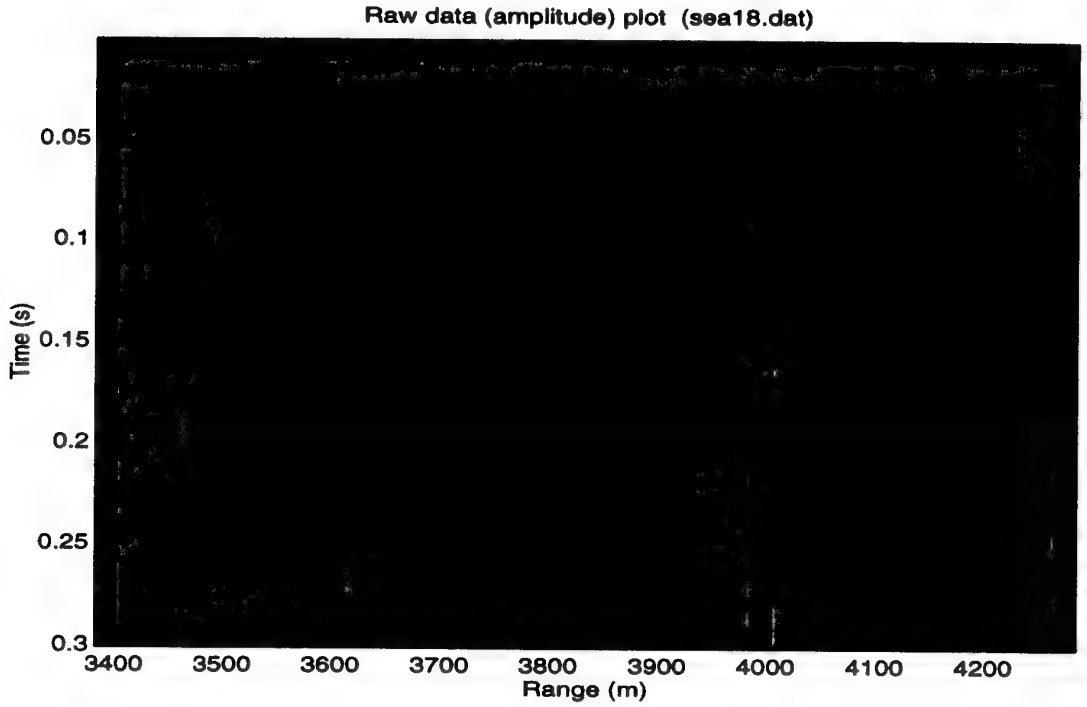

Figure 5 Experimentally collected sea clutter

Figure 6 presents the averaged temporal (for the speckle component) and spatial (for the Gamma component) autocorrelation functions for the data set. At any range, the return fluctuates with a time constant of approximately 10 ms as the scatterers within the patch move with the internal motion of the sea and change their phase relations. The local mean level varies with range owing to bunching of the scatterers. The correlation length of the sea surface in the range direction is about 6.5 m. The duration (0.3 s) of the data collection is not sufficient for the bunching to change at any given range.

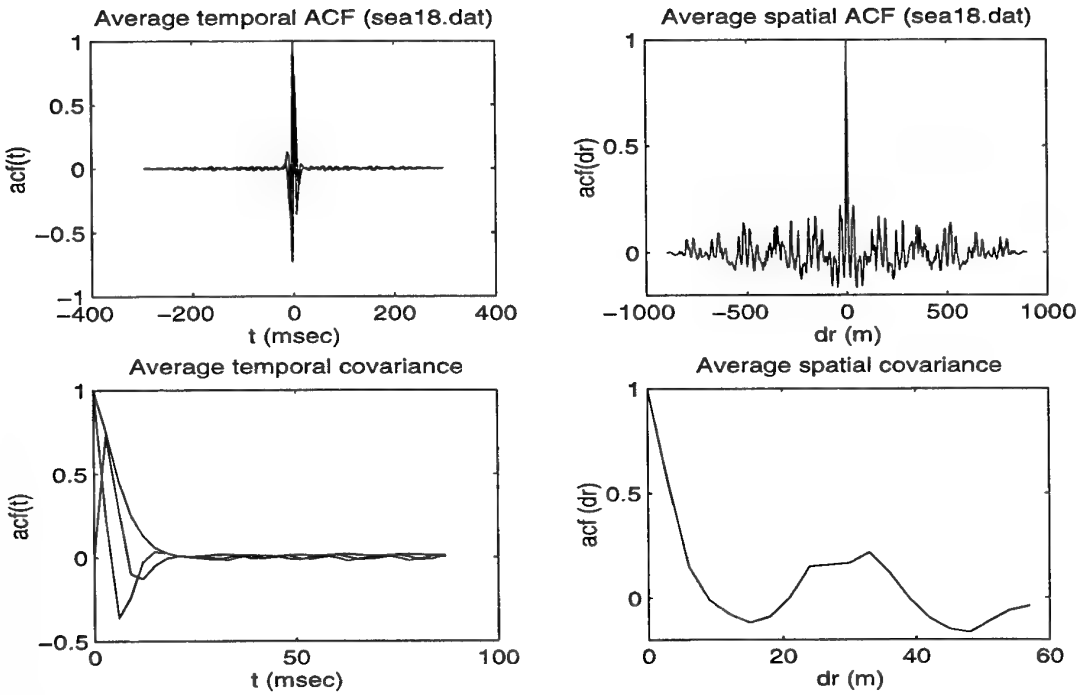

Figure 6 Temporal and spatial autocorrelation functions for experimentally collected sea clutter

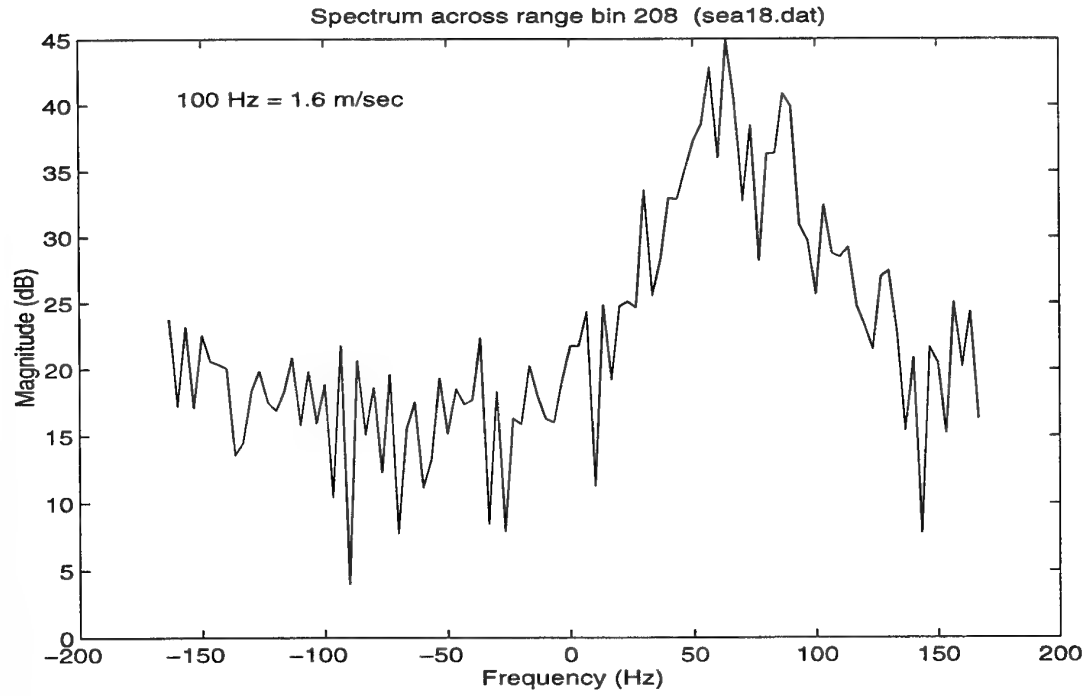

Figure 7 Spectral analysis for the range bin of experimentally collected sea clutter

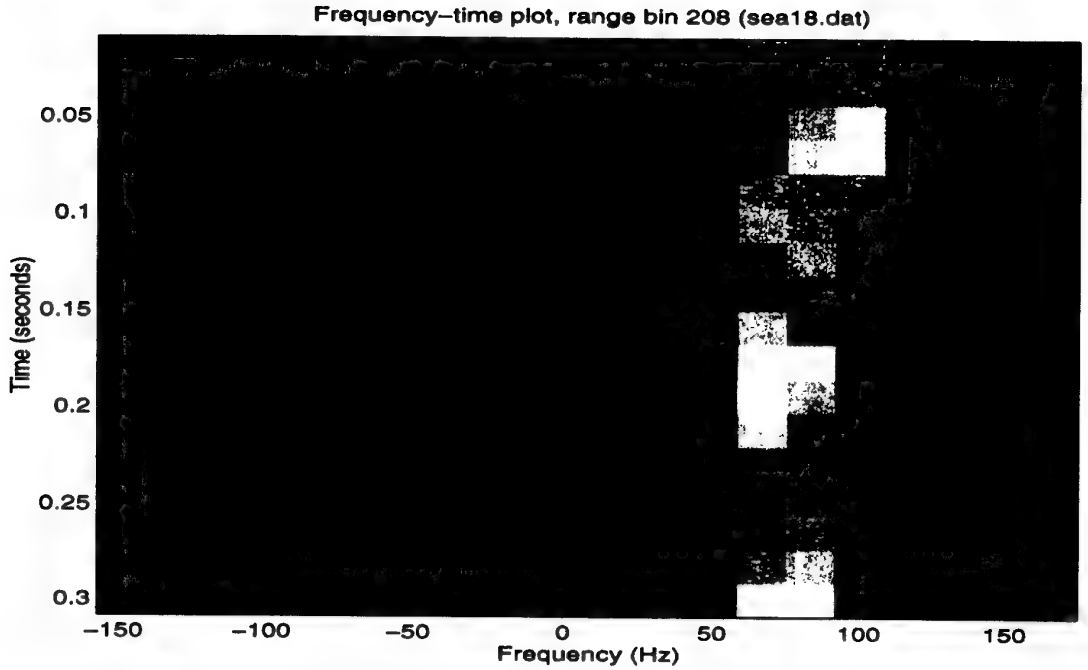

Figure 8 Frequency-time analysis for the range bin of experimentally collected sea clutter

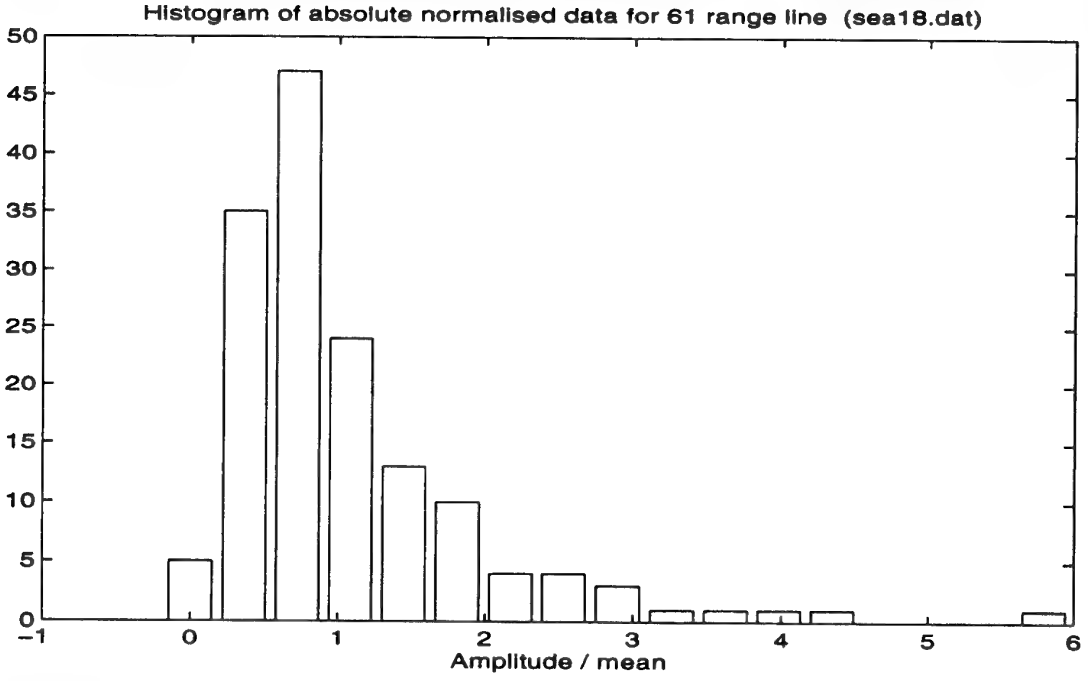

Figure 9 Normalised amplitude histogram for a range line of experimentally collected sea clutter

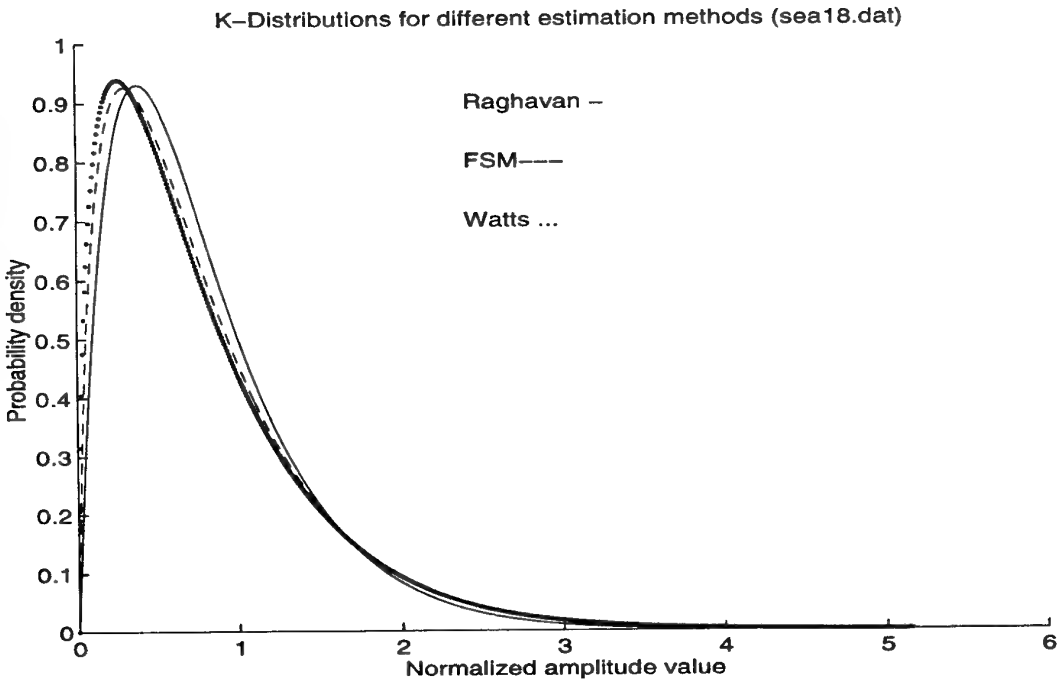

Figure 10 K-PDFs estimated by different methods for experimentally collected sea clutter

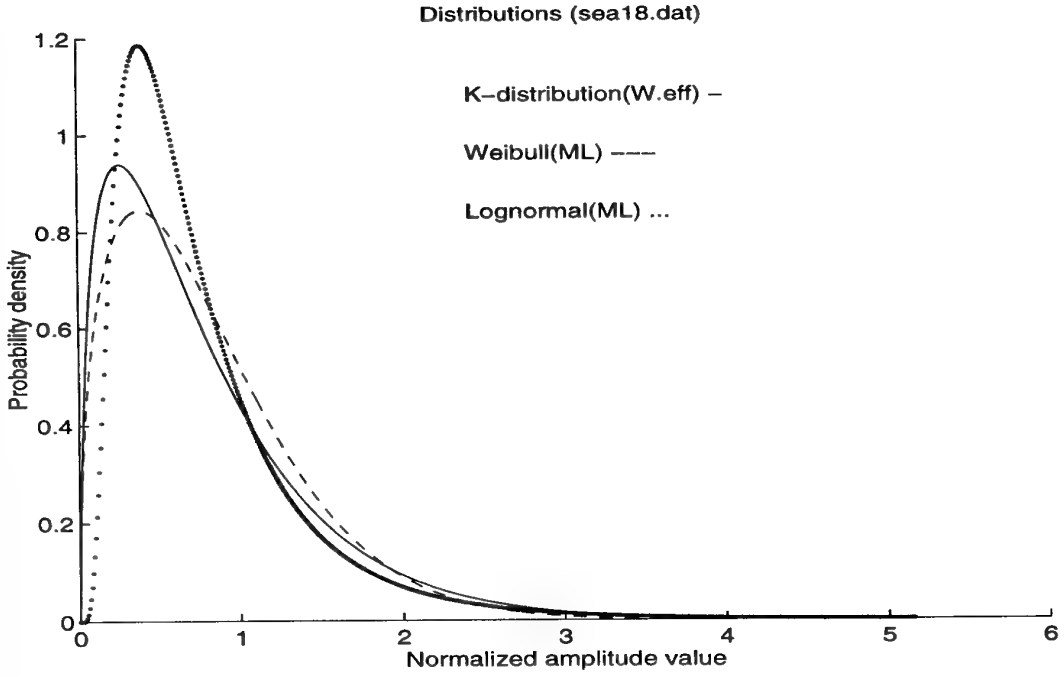

Figure 11 PDFs of different distributions for experimentally collected sea clutter

Figure 7 presents the results of spectral analysis of the range bin of the image with the largest value of amplitude of the echo signals, figure 8 is an image plot of frequency-time analysis (20 points FFTs) for the same data.

Figure 9 is a plot of the normalised histogram of the amplitude returns. Figure 10 is a plot of the probability density functions for the K-distribution estimated by Watts's, first and second moments (FSM), and Raghavan's methods [20]. Figure 11 is a plot of the probability density functions for the Log-Normal and Weibull distributions estimated by the maximum likelihood (ML) method and the K-distribution estimated by Watts's method.

Table 4 lists estimates of the parameters for the K-distribution by using these three methods (Watts's, first and second moments (FSM) and Raghavan's) as well as estimates of the parameters for the Log-Normal and Weibull distributions from the ML method.

As each calculated parameter was averaged through all realisations (each realisation presents the echo signals from 300 range bins), the presented results are the mean values of these parameters.

Table 4 Estimates of the distribution parameters by different methods for experimentally collected sea clutter data set

Parameter	L	W(ML)	K(R)	K(W)	K(FSM)
ν	(μ) -0.53	(γ) 1.3826	1.4110	0.8778	1.0077
c	(σ^2) 0.6243	(ϖ) 0.8617	2.4441	1.8473	1.9953

The different methods for estimation of the K-distribution parameters produce quite different estimates of the parameters. The reason for this is the low clutter to noise ratio (CNR =10.7 dB) for the experimentally collected data set. The presence of quite strong thermal noise in the radar receiver modifies the distribution of the received signals significantly. It is known [20] that in this case it may be advisable the usage modified Watts's method for estimation purposes. Unfortunately, this method requires a sufficiently large number of independent samples to estimate the higher moments accurately. Instead, we calculate the K-distribution parameters Watts's method without modifications, estimating the effective value of the shape parameter, related to the true value by

$$\nu_{eff} = \nu\left(1+\frac{1}{CNR}\right)^2 , \qquad (51)$$

where CNR is the clutter to noise ratio.

This method provides a reasonable fit to the tail of the data with added noise, but give a poor fit for the low amplitude values. Because the tail region is responsible for such an important detection characteristic as probability of false alarm, from the point of view of practical radar applications the moments methods are better in low CNR situations. The presented results of the statistical analysis are in agreement with this statement: in the low false alarm region Watts's method gives the best results.

Table 5 lists the modified chi-squared index χ_m^2 values [4] for all these distributions and the standard deviation σ_v of the estimates of the K-distribution shape parameter by each method.

The comparison of the modified chi-squared index χ_m^2 values for all the distributions shows that the best results in the important tail area can be achieved by applying the K-distribution model to the sea clutter. Among the K-distribution parameters estimation methods, the distribution with the parameters using Watts's method gives a better fit in this region to the experimentally collected data histogram than the others.

Table 5 Modified chi-squared index χ_m^2 values and standard deviation σ_v for different estimation methods for experimentally collected sea clutter data set

Parameter	L	W(ML)	K(R)	K(W)	K(FSM)
χ_m^2	516.7934	164.7579	180.7605	123.7512	130.5519
σ_v			0.3654	0.3349	0.2596

Analysis of the standard deviation σ_v of the estimates of the K-distribution shape parameter by each method shows that the FSM method has a smaller deviation than Watts's method, which can be explained by smaller variability in the lower-order sample moments. Quite a big value of the standard deviation for Raghavan's method follows from the fact that it gives a good fit to the lower amplitude values, which are the most distorted by noise.

Synthetic generation of sea clutter returns was implemented for the radar system with the same parameters. Estimated parameters for the experimentally collected data set , which were used as input parameters for the simulation procedures, are:

- CNR = 10.7 dB. This value was calculated for the GIT model of the mean clutter reflectivity, and the radar and environmental parameters in which the data set has been collected;

- the K-distribution shape parameter $\nu = 0.74$. This value was calculated from equation (51), using the estimated values of the effective shape parameter ν_{eff} and the CNR;

- the K-distribution scale parameter c = 1.72 for normalised data, having unit second sample moment , was calculated using relation (5);

- the average Doppler frequency f_d = 65 Hz;

- the one-lag correlation coefficient ρ_t = 0.87 for the temporal autocorrelation function, presented by (46);

- the one-lag correlation coefficient ρ_r = 0.56 for the spatial autocorrelation function, presented by (47).

The results of this simulation and their analysis are presented in Figure 12 to Figure 17 for a realisation of the synthetically generated process.

The simulated data set consists of 100 consecutive pulses sampled at 300 range bins, totalling 30,000 sample points. The synthetically generated data has been normalised to have unit second sample moment.
Figure 12 provides a crude image of the amplitude returns for the simulated sea clutter.

Figure 13 presents the averaged temporal and spatial autocorrelation functions for this synthetically generated data set. Figures 6 and 13 show similarity of the temporal and spatial correlation properties of experimentally collected and synthetically generated sea clutter data sets. At the same time, the temporal characteristics of the data sets are in a closer agreement to each other than the spatial characteristics. The difference can be explained by the usage of the nonlinear transformation procedure for the simulation of specified spatial correlation properties of the K-distributed sea clutter with arbitrary value of the shape parameter. This procedure is necessary in order to generate the sea clutter data with chosen spatial correlation properties within reasonable computation time but adds some inaccuracy to the results.

Figure 14 presents the results of spectral analysis for the range bin of the synthetically generated image with the largest value of amplitude of echo signals. Figure 15 is image plot of frequency-time analysis (20 points FFTs) for this range bin. Comparison of the spectral characteristics of the synthetically generated data (Figure 14, 15) to those of the experimentally collected data (Figure 7, 8) shows that they are very similar to each other as well.

Figure 16 is a plot of the normalised histogram of the simulated amplitude returns. The form and parameters of the histograms of the synthetically generated and experimentally collected data sets (Figures 16 and 9, respectively) are quite close to each other.

Table 6 lists estimates of the parameters for the K-distribution calculated by using the three methods: Watts's, Raghavan's and first and second moments.

Table 6 Estimates of the K-distribution parameters by different methods for synthetically generated sea clutter data set

Parameter	K(R)	K(W)	K(FSM)
ν	1.3297	0.9958	1.0396
c	2.3530	1.9453	2.0210

Figure 17 is a plot of the probability density functions for the K-distribution estimated by Watts's, first and second moments (FSM) and Raghavan's methods [20].

Comparison of the results for the estimates of the K-distribution parameters for the experimentally collected and synthetically generated data sets (Tables 4 and 6, respectively) shows a smaller variance in the values of the estimated parameters in the case of the generated data. The reasons of such a difference are:

- sensitivity of Watts's estimation method of the K-distribution parameters to the limited number of independent samples;

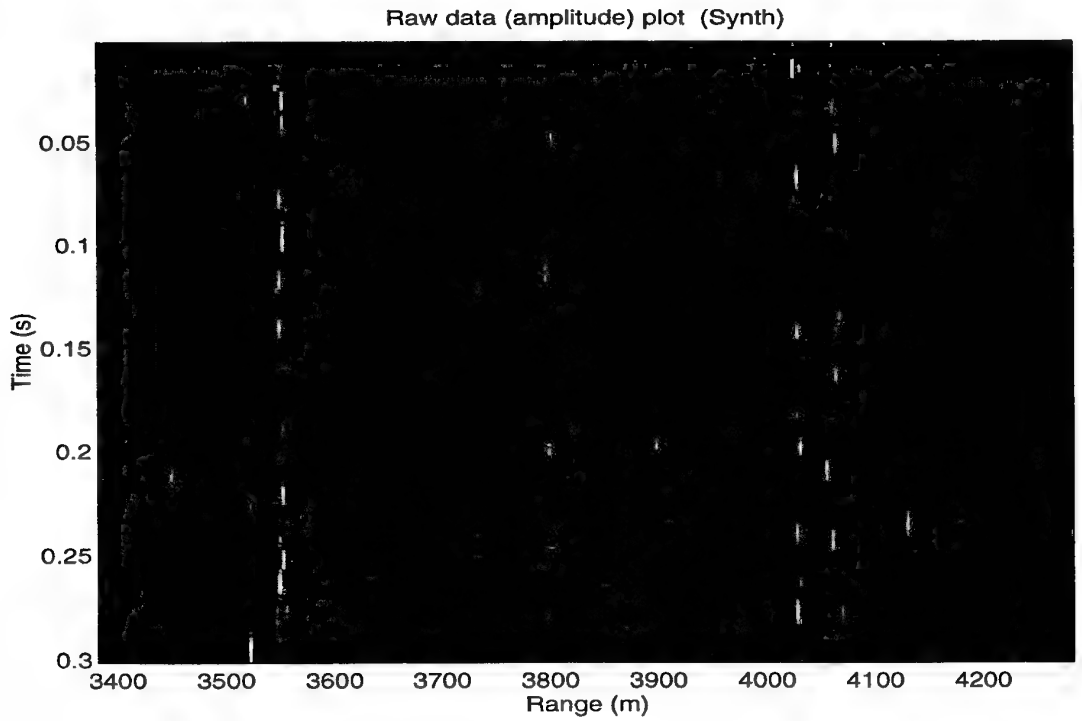

Figure 12 Synthetically generated sea clutter

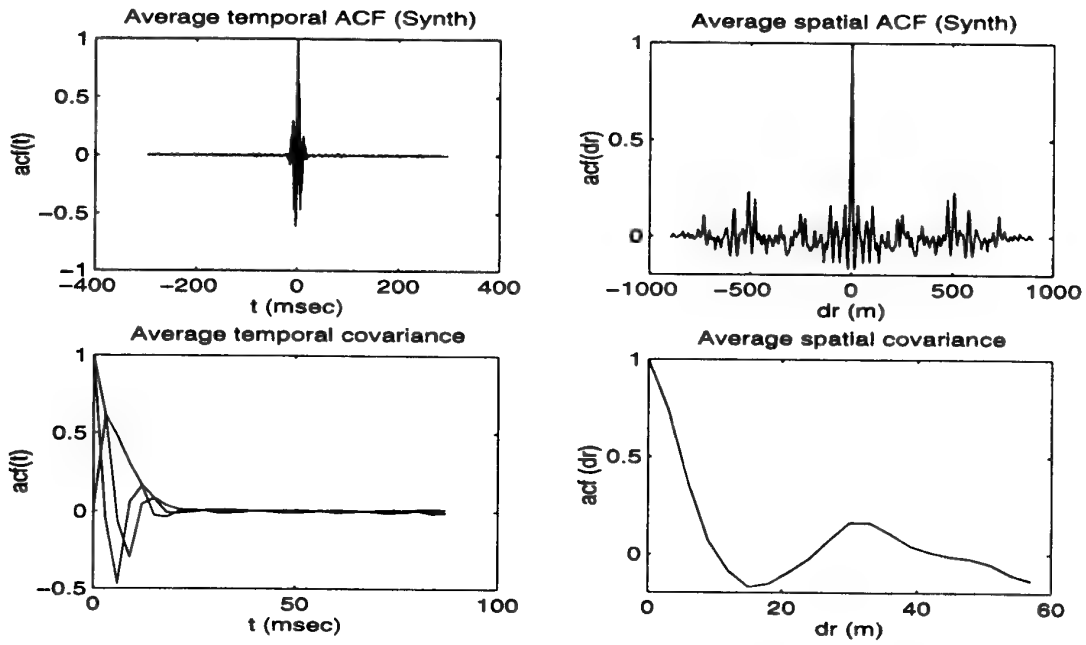

Figure 13 Temporal and spatial autocorrelation functions for synthetically generated sea clutter

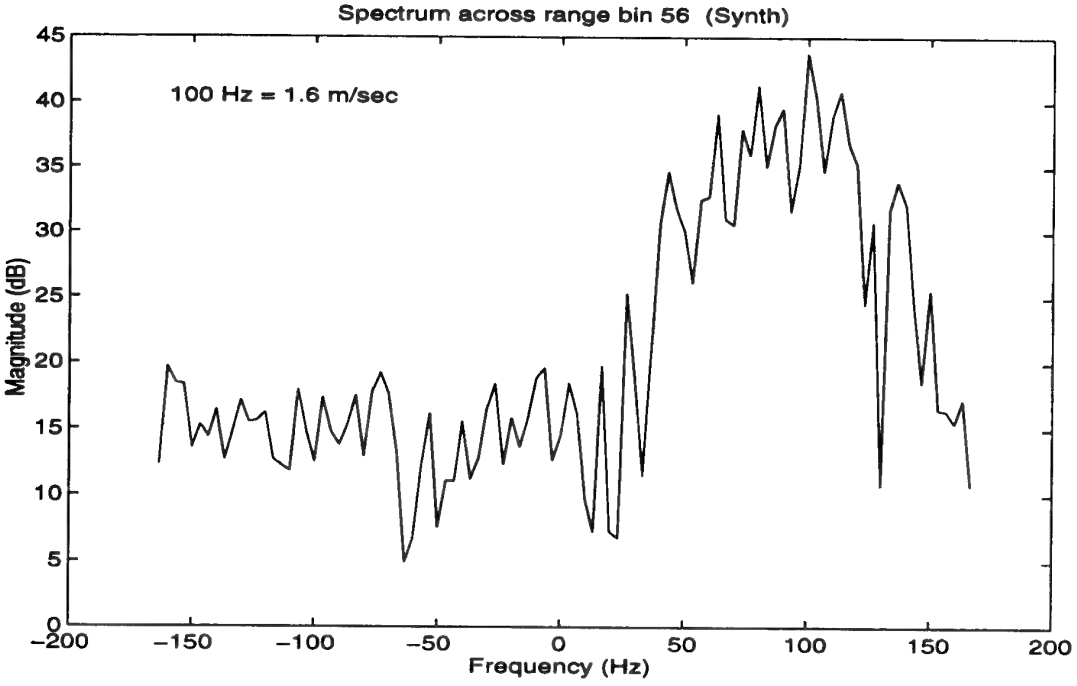

Figure 14 Spectral analysis for the range bin of synthetically generated sea clutter

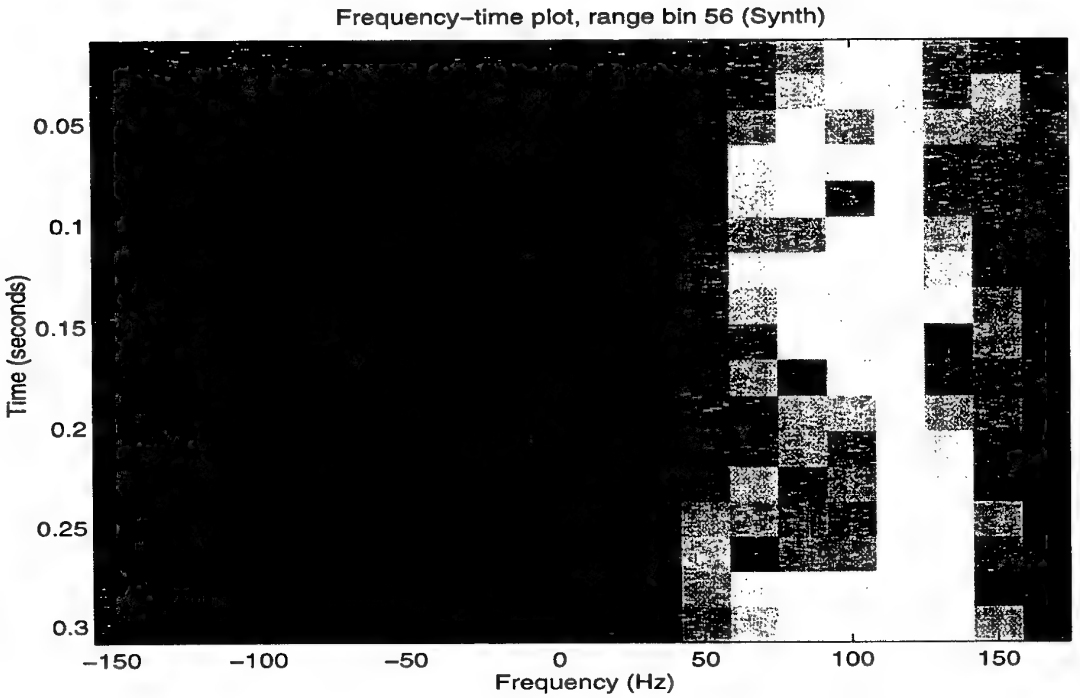

Figure 15 Frequency-time analysis for the range bin of synthetically generated sea clutter

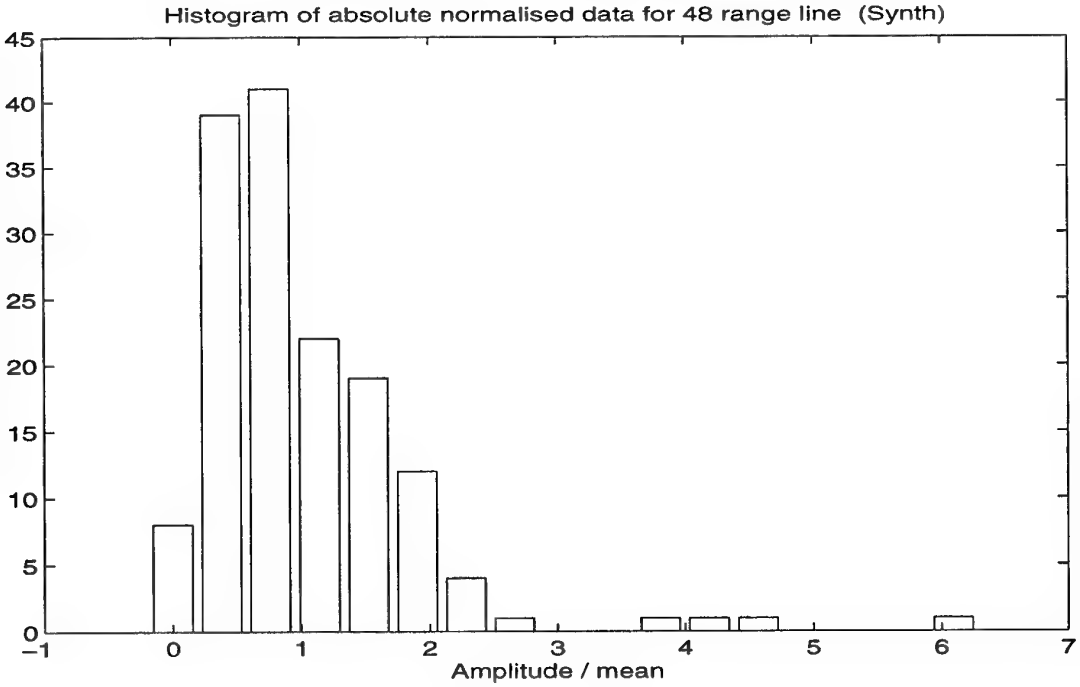

Figure 16 Normalised amplitude histogram for a range line of synthetically generated sea clutter

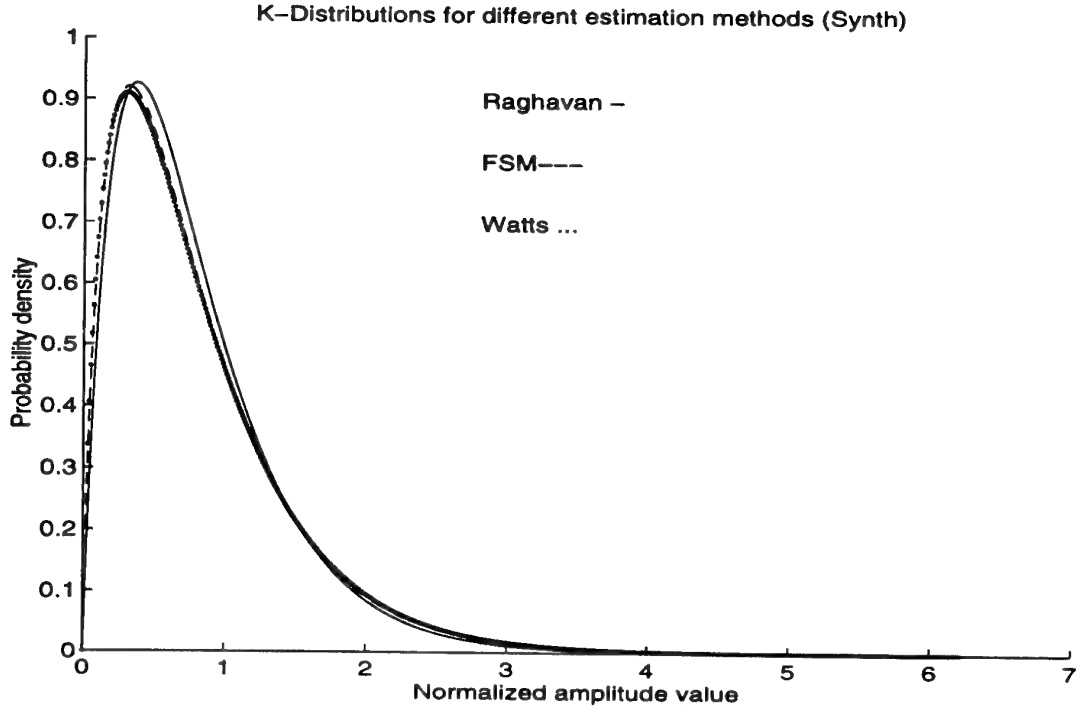

Figure 17 K-PDFs estimated by different methods for synthetically generated sea clutter

- inability to accurately estimate the CNR using the experimentally collected data, because of the limited number of independent samples, leading to the necessity to calculate the expected CNR using one of the mean clutter reflectivity models;
- inaccuracy of estimation and prediction of some of the parameters, which are needed in the sea clutter simulation, as a result of the low clutter to noise ratio;
- the usage of the nonlinear transformation procedure for the simulation of specified spatial correlation properties of the K-distributed sea clutter with arbitrary value of the shape parameter.

Table 7 lists the modified chi-squared index χ_m^2 values and standard deviation σ_v for each of these methods.

Table 7 Modified chi-squared index χ_m^2 values and standard deviation σ_v for different estimation methods for synthetically generated sea clutter data set

Parameter	K(R)	K(W)	K(FSM)
χ_m^2	165.7917	133.7698	135.9418
σ_v	0.3611	0.4839	0.3145

The values of the parameters, presented in Table 7 for the synthetically generated data, are in a good agreement with those for the K-distribution model of the experimentally collected data, presented in Table 4.

The comparison of the analysis results for the experimentally collected and synthetically generated sea clutter data shows that the combination of the previously described in this report procedures for modelling of the K-distributed sea clutter provides a means of achieving good results in the simulation of sea clutter returns with the desired parameters of the amplitude distribution and the specified correlation properties.

5. Summary

This report presents some results of a study of sea clutter characteristics prediction and simulation of K-distributed sea clutter with specified amplitude distribution and specified temporal and spatial correlation properties. The analysis and comparison of the experimentally collected and synthetically generated data show that the K-distribution is the most promising model of sea clutter which enables simulation of clutter with a good level of approximation to the real data.

For the successful implementation of the suggested sea clutter characteristics prediction and K-distributed sea clutter simulation procedures for a radar system operating in Australian environmental conditions, several problems have to be solved in the future such as:

- clarification of which sea clutter model among the existing models (SIT, GIT, TSC, HYB) provides the best results for Australian environmental conditions;

- validation of the existing empirical models for prediction of the shape parameter of the K-distribution for a radar range resolution less than 4m;

- clarification of the effect of pulse compression on the predicted value of the shape parameter of the K-distribution.

Simulators based on the developed models can be used to generate realistic sea clutter data which can be input to computer models of the radar system and the resulting performance measured.

6. References

1. Hou, X.-Y., and Morinaga, N. "Detection performance in K-distributed and correlated Rayleigh clutters", IEEE Trans. AES, Vol.25, No 5, Sept. 1989, pp. 634-641.

2. Nathanson, F.E. "Radar design principles", McGraw-Hill Book Co., 1969.

3. Nathanson, F.E., Reilly, J.P., and Cohen, M.N. "Radar design principles: signal processing and the environment", 2nd ed., McGraw-Hill inc., 1990.

4. Chan, H.C. "Radar sea clutter at low grazing angles", IEE Proc., Vol. 137, Pt. F, No 2, Apr. 1990, pp. 102-112.

5. Peebles, P.Z. "The generation of correlated log-normal clutter for radar simulations", IEEE Trans. AES, Vol. 7, No 6, Nov. 1971, pp. 1215-1217.

6. Szajnowski, W.J. "Generation of correlated log-normal clutter samples", Electronic Letters, Vol. 12, No 19, Sept. 16 1976, pp. 497-498.

7. Farina, A., Russo, A., and Studer, F.A. " Coherent radar detection in log-normal clutter", IEE Proc., Vol. 133, Pt. F, No 1, Feb. 1986, pp. 39-54.

8. Conte, E., and Longo, M. "On a coherent model for log-normal clutter", IEE Proc., Vol. 134, Pt. F, No 2, Apr. 1987, pp. 198-201.

9. Szajnowski, W.J. "The generation of correlated Weibull clutter for signal detection problems", IEEE Trans. AES, Vol. 13, No 5, Sept. 1977, pp. 536-540.

10. Farina, A., Russo, A., Scannapieco, F., and Barbarossa, F. "Theory of radar detection in coherent Weibull clutter", IEE Proc., Vol. 134, Pt. F, No 2, Apr. 1987, pp. 174-190.

11. Li, G., and Yu, K.-B. "Modelling and simulation of coherent Weibull clutter", IEE Proc., Vol 136, Pt. F, No 1, Feb. 1989, pp. 2-12.

12. Rifkin, R. "Analysis of CFAR performance in Weibull clutter", IEEE Trans. AES, Vol. 30, No 2, Apr. 1994, pp. 315-328.

13. Azzarelli, T. "General class of non-Gaussian coherent clutter models", IEE Proc., Vol. 142, Pt. F, No 2, Apr. 1995, pp. 61-70.

14. Marier, I.J. "Correlated K-distributed clutter generation for radar detection and track", IEEE Trans. AES, Vol. 31, No 2, Apr. 1995, pp.568-580.

15. Baker, C.J. "K-distributed coherent sea clutter", IEE Proc., Vol. 138, Pt. F, No 2, Apr. 1991, pp. 89-92.

16. Nohara, T.J., and Haykin, S. "Canadian East Coast radar trial and the K-distribution", IEE Proc., Vol. 138, Pt. F, No 2, Apr. 1991, pp. 80-88.

17. Ward, K.D., Baker, C.J., and Watts, S. "Maritime surveillance radar. Part 1: Radar scattering from the ocean surface", IEE Proc., Vol. 137, Pt. F, No 2, Apr. 1990, pp. 51-62.

18. Ward, K.D., Baker, C.J., and Watts, S. "Maritime surveillance radar. Part 2: Detection performance prediction in sea clutter", IEE Proc., Vol. 137, Pt. F, No 2, Apr. 1990, pp. 63-72.

19. Raghavan, R.S. " A method for estimating parameters of K-distributed clutter", IEEE Trans. AES, Vol. 27, No 2, March 1991, pp. 238-246.

20. Joughin, I.R., Percival, D.B., and Winebrenner, D.P. "Maximum likelihood estimation of K-distribution parameters for SAR data", IEEE Trans. Geosci. Remote Sensing, Vol. 31, 1993, pp. 989-999.

21. Watts, S. " A practical approach to the prediction and assessment of radar performance in sea clutter", IEEE International Radar Conference, 1995, pp. 181-186.

22. Ryan, J. and Johnson, M. "Modelling radar sea clutter", For Defence Research Establishment Ottawa, Contract Report, W7714-9-9257/01-ST, 1990, pp. 1-62.

23. Sittrop, H., "On the sea-clutter dependency on windspeed", Radar-77, IEE Conf. Proc. No 155, London, England, 1977, pp. 110-114.

24. Horst, M.M., Dyer, F.B., and Tuley, M.T. "Radar sea clutter model", URSI Digest, 1978 Int. IEEE AP/S URSI Symp., College Park, Maryland, USA, pp. 6-10.

25. Technology Service Corporation, 1990, "Section 5.6.1: Backscatter from sea", Radar Workstation, Vol. 2, pp. 177-186.

26. Reilly, J.P., Dockery, G.D. "Influence of evaporation ducts on radar sea return", IEE Proc., Vol. 137, Pt. F, No 2, Apr. 1990, pp. 80-88.

27. Barton, D.K. "Radars", Vol.5, The Raytheon Co., 1975.

28. Dockery, G.D. "Method for modelling sea surface clutter in complicated propagation environments, IEE Proc., Vol. 137, Pt. F, No 2, Apr. 1990, pp. 73-79.

29. Helmken, H.F. "Low-grazing-angle radar backscatter from the ocean surface", IEE Proc., Vol. 137, Pt. F, No 2, Apr. 1990, pp. 113-117.

30. Paulus, R.A. "Evaporation duct effects on sea clutter", IEEE Trans. AP, Vol. 38, No 11, Nov. 1990, pp. 1765-1771.

31. Ward, K.D. "A radar sea clutter model and its application to performance assessment", Radar-82, pp. 203-207.

32. Watts, S., Wicks, D.C. "Empirical models for prediction in K-distribution radar sea clutter", IEEE Internat. Radar Conf., 1990, pp. 189-194.

33. Watts, S., and Ward, K.D. "Spatial correlation in K-distributed sea clutter", IEE Proc., Vol. 134, Pt. F, No 2, Apr. 1987, pp. 526-531.

34. Ryan, J. and Johnson, M. "Radar performance prediction for target detection at sea", Radar-92, IEE Conf. Proc. No 365, 1992, pp. 13-17.

35. Lombardo, P., Oliver, C.J. "Estimating the correlation properties of K-distributed SAR clutter", IEE Proc., Radar, Sonar Navig., Vol. 142, No 4, Aug. 1995, pp. 167-178.

36. Raghavan, R.S. "A model for spatially correlated radar clutter", IEEE Trans. AES, Vol. 27, No 2, March 1991, pp. 268-275.

37. Conte, E., Galati, G., and Longo, M. "Exogenous modelling of non-Gaussian clutter", J.Inst.Electron. and Radio Eng., 1987, Vol. 57, No 4, pp. 191-197.

38. Conte, E., and Longo, M. "Characterisation of radar clutter as a spherically invariant random process", IEE Proc., Vol. 134, Pt. F, No 2, Apr. 1987, pp. 191-197.

39. Conte, E., Longo, M., and Lops, M. "Modelling and simulation of non-Rayleigh radar clutter", IEE Proc., Vol. 138, Pt. F, No 2, Apr. 1991, pp. 121-130.

40. Rangaswamy, M, Weiner, D., and Ozturk, A. "Non-Gaussian random vector identification using spherically invariant random processes", IEEE Trans. AES, Vol. 29, No 1, Jan 1993, pp. 111-123.

41. Rangaswamy, M, Weiner, D., and Ozturk, A. "Computer generation of correlated non-Gaussian radar clutter", IEEE Trans. AES, Vol. 31, No 1, Jan 1995, pp. 106-116.

42. Conte, E., Longo, M., Lops, M., and Ullo, S.L. "Radar detection of signals with unknown parameters in K-distributed clutter", IEE Proc., Vol. 138, Pt. F, No 2, Apr. 1991, pp. 131-138.

43. Armstrong, B.C., and Griffiths, H.D. "CFAR detection of fluctuating targets in spatially correlated K-distributed clutter", IEE Proc., Vol. 138, Pt. F, No 2, Apr. 1991, pp. 139-152.

44. Oliver, C.J., and Tough, R.J.A. " On the simulation of correlated K-distributed random clutter", Optica Acta, 1986, No 33, pp. 223-250.

45. Blacknell, D. "New method for the simulation of correlated K-distributed clutter", IEE Proc., Radar, Sonar Navig., Vol. 141, 1994, pp. 53-58.

46. Armstrong, B.C., and Griffiths, H.D. "Modelling spatially correlated K-distributed clutter", Electronic Letters, 18th July, 1991, Vol. 27, No 15, pp. 1355-1356.

47. Watts, S. "Radar detection prediction in K-distributed sea clutter and thermal noise", IEEE Trans. AES, Vol. 23, No 1, Jan 1987, pp. 40-45.

Appendix 1
SIT Sea Clutter Model

The average radar cross-section per unit area σ_0 (in $\mathrm{dB}m^2/m^2$) is given by the expression

$$\sigma_0 = \alpha + \beta \log\frac{\varphi}{\varphi_0} + [\delta \log\frac{\varphi}{\varphi_0} + \gamma]\log\frac{W_v}{W_0}, \qquad (1.1)$$

where

φ_0 and W_0 are respectively the reference grazing angle in degrees and the reference wind velocity in knots;

φ and W_v are respectively the grazing angle and the wind speed for which the clutter is described;

α, β, γ and δ are constants derived from the experiments.

The values of the reference parameters and the constants for wave length λ=3.2 cm (X-band) are given in Table 8.

Table 8 Sittrop's sea clutter model constants

Wind direction	Polaris.	φ_0 degrees	W_0 kts.	α dB	β dB	γ dB	δ dB
upwind	hor.	0.5	10	-50	12.6	34	-13.2
crosswind	hor.	0.5	10	-53	6.5	34	0
upwind	vert.	0.5	10	-49	17	30	-12.4
crosswind	vert.	0.5	10	-58	19	50	-33

Appendix 2
GIT Sea Clutter Model

1. Frequency range =1 to 10 GHz

a) Interference factor:

$$\sigma_\varphi = (14.4\lambda + 5.5)\varphi h_{av}/\lambda\,, \tag{2.1}$$

$$A_I = \sigma_\varphi^4/(1+\sigma_\varphi^4)\,, \tag{2.2}$$

where λ is the radar wavelength (m), φ is the grazing angle (radians) and h_{av} is the average wave height (m).

b) Upwind/downwind factor:

$$A_u = \exp\{0.2\cos\phi(1-2.8\varphi)(\lambda+0.02)^{-0.4}\} \tag{2.3}$$

where ϕ is the look direction relative to wind direction angle (radians).

c) Wind speed factor:

$$qw = 1.1/(\lambda+0.02)^{0.4}\,, \tag{2.4}$$

$$A_W = [1.94V_W/(1+V_W/15.4)]^{qw}\,, \tag{2.5}$$

where V_W is the wind speed which must be input separately for the conditions of changing wind and is given by

$$V_W = 8.67h_{av}^{0.4} \tag{2.6}$$

for a "fully arisen" sea under conditions of stationary equilibrium.

d) Reflectivity (in dB m^2/m^2):

1) Horizontal polarisation

$$\sigma_0(H) = 10\log(3.9*10^{-6}\lambda\varphi^{0.4}A_I A_u A_W)\,, \tag{2.7}$$

2) Vertical polarisation

$$\sigma_0(V) = \begin{cases} \sigma_0(H) - 1.05\ln(h_{av} + 0.015) + 1.09\ln(\lambda) + 1.27\ln(\varphi + 0.0001) + 9.70, \\ \qquad 3GHz < f < 10GHz \\ \sigma_0(H) - 1.73\ln(h_{av} + 0.015) + 3.76\ln(\lambda) + 2.46\ln(\varphi + 0.0001) + 22.2, \\ \qquad f < 3GHz \end{cases} \tag{2.8}$$

2. Frequency range =10 to 100 GHz

a) Interference factor:

$$\sigma_\varphi = (14.4\lambda + 5.5)\varphi h_{av}/\lambda, \tag{2.9}$$

$$A_f = \sigma_\phi^4/(1+\sigma_\phi^4), \tag{2.10}$$

b) Upwind/downwind factor:

$$A_u = \exp\{0.25\cos\phi(1 - 2.8\varphi)\lambda^{-0.33}\} \tag{2.11}$$

c) Wind speed factor:

$$qw = 1.93\lambda^{-0.04}, \tag{2.12}$$

$$A_W = [1.94V_W/(1+V_W/15.4)]^{qw}, \tag{2.13}$$

where V_W is the wind speed which must be input separately for the conditions of changing wind and is given by

$$V_W = 8.67h_{av}^{0.4} \tag{2.14}$$

for a "fully arisen" sea under conditions of stationary equilibrium.

d) Reflectivity (in dB m^2/m^2):

1) Horizontal polarisation

$$\sigma_0(H) = 10\log(5.78 * 10^{-6}\varphi^{0.547}A_f A_u A_W), \tag{2.15}$$

2) Vertical polarisation

$$\sigma_0(V) = \sigma_0(H) - 1.38\ln(h_{av}) + 3.43\ln(\lambda) + 1.31\ln(\varphi) + 18.55 \tag{2.16}$$

Appendix 3
TSC Sea Clutter Model

The equations used for the low grazing angle are:

a) Low grazing angle factor:

$$\sigma_z = 0.115 S^{1.95}, \tag{3.1}$$

$$\sigma_\alpha = 14.9\varphi(\sigma_z + 0.25)/\lambda, \tag{3.2}$$

$$G_A = \sigma_\alpha^{1.5}/(1+\sigma_\alpha^{1.5}), \tag{3.3}$$

where λ is the radar wavelength (ft), φ is the grazing angle (radians), S is the sea state and σ_z is the surface height standard deviation.

b) Wind speed factor:

$$V_W = 6.2 S^{0.8}, \tag{3.4}$$

$$Q = \varphi^{0.6}, \tag{3.5}$$

$$A_1 = (1+(\lambda/0.03)^3)^{0.1}, \tag{3.6}$$

$$A_2 = (1+(\lambda/0.1)^3)^{0.1}, \tag{3.7}$$

$$A_3 = (1+(\lambda/0.3)^3)^{Q/3}, \tag{3.8}$$

$$A_4 = 1+0.35Q, \tag{3.9}$$

$$A = 2.63\, A_1/(A_2 A_3 A_4), \tag{3.10}$$

$$G_W = [(V_W + 4.0)/15]^A, \tag{3.11}$$

c) Aspect factor:

$$G_u = \begin{cases} 1, \varphi = \pi/2 \\ \exp(0.3\cos\phi * \exp(-\varphi/0.17)/(\lambda^2 + 0.005)^{0.2}), otherwise' \end{cases} \tag{3.12}$$

where V_W is the wind speed and ϕ is the look direction relative to wind direction angle (radians).

d) Reflectivity (in m^2/m^2):

1) Horizontal polarisation

$$\sigma_0(H) = 1.7 * 10^{-5} \varphi^{0.5} G_u G_W G_A / (\lambda + 0.05)^{1.8}, \tag{3.13}$$

2) Vertical polarisation

$$10\log(\sigma_0(V)) = \begin{cases} 10\log(\sigma_0(H)) - 1.73\ln(2.507\sigma_z + 0.05) + 3.76\ln\lambda + \\ \quad 2.46\ln(\sin\varphi + 0.0001) + 19.8, f < 2GHz \\ 10\log(\sigma_0(H)) - 1.05\ln(2.507\sigma_z + 0.05) + 1.09\ln\lambda + \\ \quad 1.27\ln(\sin\varphi + 0.0001) + 9.65, f \geq 2GHz \end{cases} \tag{3.14}$$

Appendix 4
HYB Sea Clutter Model

The reflectivity (in dB m^2/m^2) is given by

$$\sigma_0 = \sigma_0(ref) + K_g + K_s + K_p + K_d, \tag{4.1}$$

where $\sigma_0(ref)$ is a reference reflectivity applying to sea state S=5, grazing angle $\varphi = 0.1^o$, vertical polarisation P=V, and upwind look direction $\phi = 0^o$; K_s, K_g, K_p, and K_d are decibel adjustments for arbitrary values of S, φ, P, and ϕ.

a) Reference reflectivity:

$$\sigma_0(ref) = \begin{cases} 24.4\log(f) - 65.2, f \le 12.5GHz \\ 3.25\log(f) - 42.0, f > 12.5GHz \end{cases}, \tag{4.2}$$

b) Grazing angle adjustment:

$$\begin{aligned} \varphi_r &= 0.1^o \\ \varphi_t &= \sin^{-1}(0.0632\lambda/\sigma_h), \end{aligned} \tag{4.3}$$

where φ_r is the reference grazing angle (in degrees), φ_t is the transitional angle (in degrees) and σ_h is the root-mean-square wave height (m) such as

$$\sigma_h = 0.031S^2. \tag{4.4}$$

1) for $\varphi_t \ge \varphi_r$

$$K_g = \begin{cases} 0, \varphi < \varphi_r \\ 20\log(\varphi/\varphi_r), \varphi_r \le \varphi \le \varphi_t \\ 20\log(\varphi_t/\varphi_r) + 10\log(\varphi/\varphi_t), \varphi_t < \varphi < 30^o \end{cases}. \tag{4.5}$$

2) for $\varphi_t < \varphi_r$

$$K_g = \begin{cases} 0, \varphi \le \varphi_r \\ 10\log(\varphi/\varphi_r), \varphi > \varphi_r \end{cases}. \tag{4.6}$$

c) Sea state adjustment:

$$K_s = 5(S-5), \tag{4.7}$$

d)Polarisation adjustment:

1) for vertical polarisation $K_p = 0$;

2) for horizontal polarisation K_p is given by

$$K_p = \begin{cases} 1.7\ln(h_{av}+0.015) - 3.8\ln(\lambda) - 2.5\ln(\varphi/57.3+0.0001) - 22.2, \\ f < 3GHz \\ 1.1\ln(h_{av}+0.015) - 1.1\ln(\lambda) - 1.3\ln(\varphi/57.3+0.0001) - 9.7, \\ 3GHz \le f \le 10GHz \\ 1.4\ln(h_{av}) - 3.4\ln(\lambda) - 1.3\ln(\varphi/57.3) - 18.6, \\ f > 10GHz \end{cases}, \tag{4.8}$$

where h_{av} is the average wave height (m) obtained from

$$h_{av} = 0.08S^2. \tag{4.9}$$

e) Wind direction adjustment:

$$K_d = (2 + 1.7\log(0.1/\lambda))(\cos\phi - 1), \tag{4.10}$$

where ϕ is the radar look angle with respect to the wind direction, defined such that ϕ=0 when looking upwind.

DISTRIBUTION LIST

Simulation of Sea Clutter Returns

Irina Antipov

AUSTRALIA

DEFENCE ORGANISATION

Task Sponsor: DGAD

S&T Program

Chief Defence Scientist
FAS Science Policy
AS Science Corporate Management
} shared copy

Director General Science Policy Development
Counsellor Defence Science, London (Doc Data Sheet)
Counsellor Defence Science, Washington (Doc Data Sheet)
Scientific Adviser to MRDC Thailand (Doc Data Sheet)
Director General Scientific Advisers and Trials/Scientific Adviser Policy and Command (shared copy)
Navy Scientific Adviser (Doc Data Sheet and distribution list only)
Scientific Adviser - Army (Doc Data Sheet and distribution list only)
Air Force Scientific Adviser
Director Trials

Aeronautical and Maritime Research Laboratory
Director
Chief of Air Operations Division Dr. C. Guy
Chief of Maritime Operations Division Dr. R. Creaser
Chief of Weapons Systems Division Dr. N. Nandagopal
Dr. N. Martin, WSD
R. Potter, WSD

Electronics and Surveillance Research Laboratory
Director
Chief of Wide Area Surveillance Division Dr. D.H. Sinnott
Chief of Electronic Warfare Division Dr. M.L. Lees
Chief of Tactical Surveillance System Division Dr. D. Gambling
Research Leader Tactical Surveillance Dr. D. Heilbronn
Head of Sensor Processing, TSSD, Dr. J. Whitrow
Task Manager B. Reid, TSSD
Author: I. Antipov, TSSD
Dr. C. Coleman, WASD

DSTO Library
Library Fishermens Bend
Library Maribyrnong
Library Salisbury (2 copies)

Australian Archives
Library, MOD, Pyrmont (Doc Data sheet only)

Capability Development Division
Director General Maritime Development (Doc Data Sheet only)
Director General Land Development (Doc Data Sheet only)
Director General C3I Development (Doc Data Sheet only)

Navy
SO (Science), Director of Naval Warfare, Maritime Headquarters Annex, Garden Island, NSW 2000. (Doc Data Sheet only)

Army
ABCA Office, G-1-34, Russell Offices, Canberra (4 copies)
SO (Science), DJFHQ(L), MILPO Enoggera, Queensland 4051 (Doc Data Sheet only)
NAPOC QWG Engineer NBCD c/- DENGRS-A, HQ Engineer Centre Liverpool Military Area, NSW 2174 (Doc Data Sheet only)

Intelligence Program
DGSTA Defence Intelligence Organisation

Corporate Support Program (libraries)
OIC TRS, Defence Regional Library, Canberra
Officer in Charge, Document Exchange Centre (DEC), 1 copy
*US Defence Technical Information Center, 2 copies
*UK Defence Research Information Centre, 2 copies
*Canada Defence Scientific Information Service, 1 copy
*NZ Defence Information Centre, 1 copy
National Library of Australia, 1 copy

UNIVERSITIES AND COLLEGES

Australian Defence Force Academy
Library
Head of Aerospace and Mechanical Engineering
Senior Librarian, Hargrave Library, Monash University
Librarian, Flinders University
Deakin University, Serials Section (M list), Deakin University Library,Geelong, 3217

OTHER ORGANISATIONS

NASA (Canberra)
AGPS
State Library of South Australia
Parliamentary Library, South Australia

OUTSIDE AUSTRALIA

ABSTRACTING AND INFORMATION ORGANISATIONS

INSPEC: Acquisitions Section Institution of Electrical Engineers
Engineering Societies Library, US
Documents Librarian, The Center for Research Libraries, US

INFORMATION EXCHANGE AGREEMENT PARTNERS

Acquisitions Unit, Science Reference and Information Service, UK
Library - Exchange Desk, National Institute of Standards and Technology, US
National Aerospace Laboratory, Japan
National Aerospace Laboratory, Netherlands

SPARES (10 copies)

Total number of copies: 64

DEFENCE SCIENCE AND TECHNOLOGY ORGANISATION
DOCUMENT CONTROL DATA

1. PRIVACY MARKING/CAVEAT (OF DOCUMENT)

2. TITLE

Simulation of Sea Clutter Returns

3. SECURITY CLASSIFICATION (FOR UNCLASSIFIED REPORTS THAT ARE LIMITED RELEASE USE (L) NEXT TO DOCUMENT CLASSIFICATION)

Document (U)
Title (U)
Abstract (U)

4. AUTHOR(S)

Irina Antipov

5. CORPORATE AUTHOR

Electronic and Surveillance Research Laboratory

PO Box 1500
Salisbury South Australia 5108

6a. DSTO NUMBER	6b. AR NUMBER	6c. TYPE OF REPORT	7. DOCUMENT DATE
DSTO-TR-0679	AR-010-560	Technical Report	June 1998

8. FILE NUMBER	9. TASK NUMBER	10. TASK SPONSOR	11. NO. OF PAGES	12. NO. OF REFERENCES
Z 9505/15/27	ADA 95/080	DGAD	58	47

13. DOWNGRADING/DELIMITING INSTRUCTIONS

Not Applicable

14. RELEASE AUTHORITY

Chief, Tactical Surveillance System Division

15. SECONDARY RELEASE STATEMENT OF THIS DOCUMENT

Approved for public release

OVERSEAS ENQUIRIES OUTSIDE STATED LIMITATIONS SHOULD BE REFERRED THROUGH DOCUMENT EXCHANGE CENTRE, DIS NETWORK OFFICE, DEPT OF DEFENCE, CAMPBELL PARK OFFICES, CANBERRA ACT 2600

16. DELIBERATE ANNOUNCEMENT

No Limitations

17. CASUAL ANNOUNCEMENT No Limitations

18. DEFTEST DESCRIPTORS

Sea clutter, algorithms, simulation, radar, P-3C aircraft

19. ABSTRACT

This report presents the results of a study, the main aim of which was proper prediction of sea clutter characteristics and modelling of sea clutter including both the temporal and spatial properties of the return signals. More detail has been given to the K-distribution as the most promising model of sea clutter which allows to simulate the clutter with a good level of approximation to the real data.